CONCEPT STUDY

CMOS detectors and a Preliminary Optical Design for "BRITE"
The BRIght Target Explorer Nano-Satellite

The study conducted under contract from
the Science Branch of the Canadian Space Agency

Contract number 9F007-046080/001/ST

CSA Technical Authority:
Alain Ouellet, Canadian Space Agency
6767 route de l'Aéroport, Saint-Hubert
Québec J3Y 8Y9
(450) 926-4773

May 5, 2005

University of Toronto, Department of Astronomy

University of Toronto Institute for Aerospace Studies
Space Flight Laboratory

Dynacon Inc.

Ceravolo Optical Systems

Principal Investigator: Dr. Slavek Rucinski
David Dunlap Observatory, University of Toronto
P.O.Box 360, Richmond Hill, Ont. L4C 4Y6.
Phone: 905-884-1396, FAX: 905-884-2672
e-mail: rucinski@astro.utoronto.ca

1. INTRODUCTION

1.1 The background

On June 1, 2004, the BRITE Science Team[1] led by the PI of this Study submitted a proposal to the Joint Committee on Space Astronomy (JCSA) to design and build a nano-satellite for astronomy called BRITE (for BRIght Target Explorer). JCSA advises the Canadian Space Agency (CSA) and is affiliated with the CASCA (the Canadian Astronomical Society or Société Cannadienne D'Astronomie). The proposal was well received by JCSA, but two areas related to technical aspects of the mission were identified as requiring additional investigation: (1) the proposed utilisation of a CMOS detector and (2) the optical design of a lens system. JCSA suggested that the Science Branch of the CSA fund a Concept Study on these subject and a small contract was granted in January 2005 to the PI of the BRITE project to conduct the necessary literature and Internet research as well as tests and measurements.

1.2. CMOS detectors

CMOS detectors are a new type of low light panoramic detectors. They are currently rapidly replacing CCD detectors in commercial (hand-held camera) applications, but have not yet been widely used as science detectors in astronomy, although they have several advantages over the CCD's and may replace the latter in years to come. The main advantages of the CMOS detectors are (1) the low power consumption and (2) the simplicity of the readout and linking to computer. CMOS detectors do not have charge-shifting circuitry and so that individual pixels can be seen by a computer as independent (in some versions addressable) memory locations. The CMOS detectors consume much less power than the CCD detectors, typically by 10 to 20 times, reducing the power requirements to the levels of 0.3 to 0.5W. In an article with the ominous title "Why CMOS Image Sensors are Poised to Surpass CCDs", Jakl (1999) already 5 years ago predicted a very rapid expansion of CMOS applications. However, the technology of CMOS manufacture has not yet solidified and is rapidly evolving with many different designs currently competing with each other. The most authoritative account by Janesick and Putnam (2003) discusses several technological solutions and states that "the CCD [can be] considered a mature technology whereas CMOS arrays have significant room for growth". Judging by his publication and Internet group activities, Janesick, who himself contributed very strongly to development of the CCDs and wrote the definitive textbook on them, now works entirely on CMOS detectors..

CMOS devices are currently made with some circuitry on the front side of the detector so that their active silicon sensors are buried at some depth, inside the structure. This sets limits on the convergence of the incoming beam and thus the f/ratio of the feeding optical system. The geometrical losses in some devices are compensated by micro-lens arrays which concentrate the light onto the active part of the sensors; such a solution may impact uniformity of the spatial sensitivity of the detector.

The other area of uncertainty is the behaviour of CMOS detectors under cooling. Most of the CMOS detectors are designed for hand-held or video cameras, or industrial imaging systems and are designed

[1] The members of the BRITE Science Team are: University of Toronto: Slavek Rucinski (PI), C. T. Bolton, Marten van Kerkwijk, Stefan Mochnacki, John Percy; Robert Zee; Université de Montréal: Anthony F.J. Moffat; McMaster University: Douglas Welch; University of British Columbia: Jaymie Matthews.

to operate at ambient temperatures. Typical ratings for operation are –10C to 0C on the cold end, and +35C to +50C on the hot end, while performance parameters are usually only available for ambient temperature (+20C or +25C). As is discussed in Section 2, initial analysis of CMOS detectors for the BRITE mission showed the dark current noise to be the performance-limiting factor, necessitating operation below 0C. By appropriate thermal design of the BRITE satellite, passive cooling of the detector showed the possibility of achieving operating temperatures between zero and –20C, a region where little performance data is available, but dark current is expected to be significantly reduced. Our study specifically addressed the thermal noise properties of typical CMOS detectors at lower temperatures than included in manufacturer specification sheets

Both, the angular sensitivity and thermal performance specifications for CMOS detectors are not published or available in any other way, so we decided to measure them for a few typical devices. The selection of representative devices for tests is described in Section 3, after an initial literature and Internet study performed by Stefan Mochnacki (Section 2). Our results are given in Section 4 (the angular sensitivity dependences) and Section 5 (the thermal and readout noise under cooling).

2.3. Optical lens system

BRITE will utilize a lens-based optical system with aperture of 25 to 35 mm diameter and focal length of 50 to 70mm (the final decision can be made only after the detector selection). The slightly larger system may be advantageous for the assumed pixel size of 8 micron as for f=70mm, the scale will be 23"/pixel. While similar lenses are made for hand-held cameras in large quantities, they usually have poor optical characteristics. Low manufacture costs are reflected – even for leading and reputable manufacturers – in strong vignetting and strongly position-dependent image distortions (resulting in a need to stop them to larger f/ratios, a requirement rarely articulated directly, but commonly employed). These deficiencies preclude use of commercial lenses in BRITE. The custom design optical system for BRITE should be vignetting-free and, because of the CMOS limitation on the f/ratio, should insure identical telecentric illumination of all points of the detector. In addition, the stellar images should be uniformly similar and sufficiently large to insure adequate sampling of the Point Spread Function (PSF), a requirement which simply cannot be assured by commercial lenses; out-of-focus images strongly accentuate poor characteristics of such lenses. The BRITE lens optics must account for the chromatic aberration over a band-pass wider than that of the Johnson V filter. While the BRITE orbit is planned to lie well below the Van Allen belts and thus cosmic ray fluxes are expected to be moderate (except for the South Atlantic Anomaly or SAA), the lenses must me free of any self-generated radioactivity or should not produce any amplification of residual cosmic ray radiation..

This study presents a preliminary optical design in Section 6. In Section 7, which goes somewhat beyond the strict goals of this study, we present sky images taken with a CMOS camera and a 50mm fixed-focus f/1.8 objective. We show there that a CMOS-based system would have ample sensitivity for BRITE, but that a commercial objective would not be sufficient for BRITE. In Section 8, conclusions of the Concept Study are presented.

2. SELECTION OF CMOS DETECTORS FOR THE STUDY

[This section on the literature and Internet research of the subject was prepared in the January 2005 by Stefan Mochnacki. It is included in the report with only minor editorial changes to explain decisions and choices concerning selection of CMOS detectors in the initial stages of this Concept Study. It retains the first person of the author.]

2.1. The background

The proposed BRITE nanosatellite has a detector power budget allowance of only 500 milli-Watts. This means that a CCD cannot be used, but CMOS detectors generally consume below 500mW, and at low readout frequencies well below that. However, an initial survey by our Dynacon colleagues showed that all the commonly-available standard OEM chips had excessive dark current, read-out noise and insufficient bits of digitization, as well as a rather small number of pixels. Typically, such CMOS chips have about 1000 – 5000 e/s/pix dark current at 20 C (close to or slightly above our expected working temperature). Even with integrations of a few seconds, the dark current becomes the dominant limitation. Readout noise of a few tens of electrons is less than the dark current noise. An excellent review of CCD and CMOS principles and the state of the art is to be found in Janesick and Putnam (2003).

While searching the Web, I found that many amateur astronomers have been using digital still cameras on telescopes. By far the best imaging of this type was being done using the Canon EOS 10D, 300D and 20D cameras, and astonishingly, these high-end cameras, with 6 to 8 megapixels, use CMOS detectors. All other high-end “Digital Single Lens Reflex” (DSLR) cameras use CCD's (as of mid-2004). I set out to investigate the performance of the Canon DSLR cameras, which can be bought for as little as C$1000.

2.2. Characteristics of DSLR cameras

There are numerous accounts in the photographic press regarding DSLR cameras; the standards for the past couple of years have been set by the Canon 10D and the Nikon D70. While each has just over 6 megapixels in a 3K × 2K with square pixels of 7 – 8 microns size, the Canon camera uses a proprietary Canon CMOS sensor, while the Nikon camera uses a Sony ICX413AQ CCD. These are colour cameras employing Bayer matrix filters: Of every group of 4 pixels, two have a G filter, one has a B and the other an R. An IR-blocking filter is mounted in front of the whole sensor, since these cameras are designed to reproduce the colour balance of the human eye.

More recently, Canon have produced a less expensive version of the 10D, called the EOS Digital Rebel or 300D, with the same detector and performance as the 10D, and an updated 8 Megapixel successor to the 10D called the 20D, while Nikon are rumoured to be producing a top-end camera with CMOS detector. There are also much more expensive and larger cameras produced by both these and other companies, but they don't appear to offer superior performance for astronomy (e.g. Canon 1D Mk. II, see Lovejoy (2004b). [Note added : Canon have announced an even better camera, the TX or 350D].

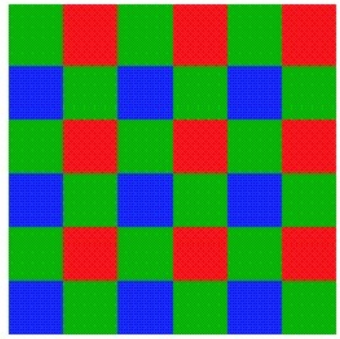

Figure 2.1: The Bayer matrix of filters over pixels.

Two amateurs have done the sort of tests needed by astronomers, Christian Buil in France and Terry Lovejoy in Australia. They publish their results on the Web. These are the tests one performs on any CCD-type detector. Buil (2004a) is well known for his development of the Audine camera, equivalent to the SBIG ST-7, both using Kodak CCD's and Lovejoy (2004a) is a knowledgeable contributor to the "digital_astro" list on Yahoo Groups.

2.3. Sensitivity or Quantum Efficiency

Unlike the full-frame charge transfer, often back-illuminated, “science grade” CCD's, the sensors in digital cameras generally have dead spaces between photosensitive pixels, leading to a fill factor less than 100%. In the case of CCD's in digital cameras, it is due to the use of inter-line transfer of charge (ILT), while in the case of CMOS detectors, there is a lot of circuitry laid down over the surface. This loss of sensitive area can be partially recovered using a matrix of microlenses bonded to the front surface.

There is another important limitation: Many sensors are colour detectors with the Bayer matrix filters mentioned above. This reduces effective quantum efficiency, and introduces geometric sampling differences between images in R, G and B, which are reduced if the image is significantly over-sampled.

2.4. Absolute QE

Lovejoy (2004a) reports crudely determined efficiencies of 0.2, 0.4 and 0.4 in the peaks of the R, G and B bands, respectively. Buil (2004b)measures the quantum efficiency of the Canon CMOS camera to be between 0.16 – 0.25 that of the Kodak KAF-402ME CCD (which at these wavelengths averages about 0.6). Thus we can expect a QE of about 0.1-0.15 for the colour CMOS chip in the Canon DSLR's. Of course, without the Bayer matrix filters, the effective quantum efficiency would be much higher, perhaps 0.5. I believe that the Canon chips have microlenses.

2.5. Relative QE

The relative QE is better established, and depends also on whether the overall IR blocking filter is removed or replaced. Blocking filter transmission curves are shown in Figure 2.2.

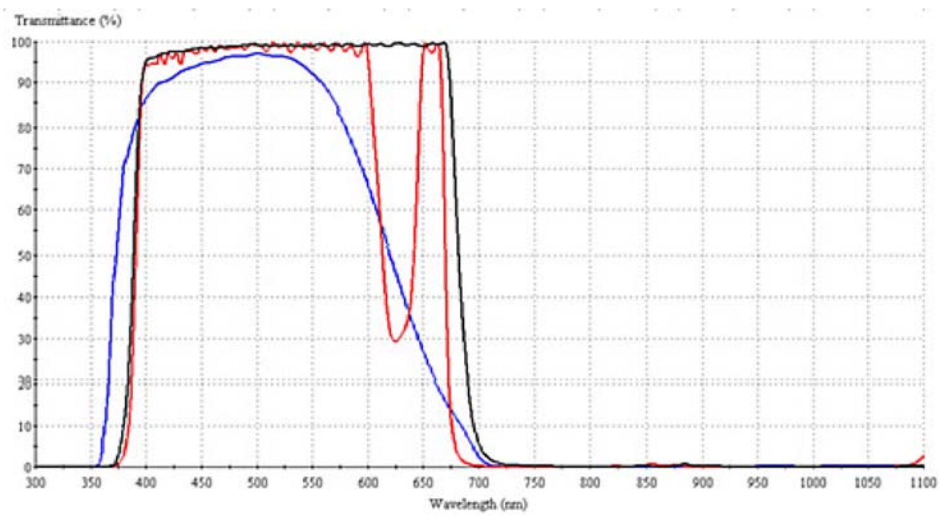

Figure 2.2: Canon IR Blocking Filter Spectral Responses.
* Blue: Original Canon IR blocker filter
* Black: Hutech Type I (used in EOS011 camera)
* Red: Hutech Type II (used in EOS012, EOS021 cameras)

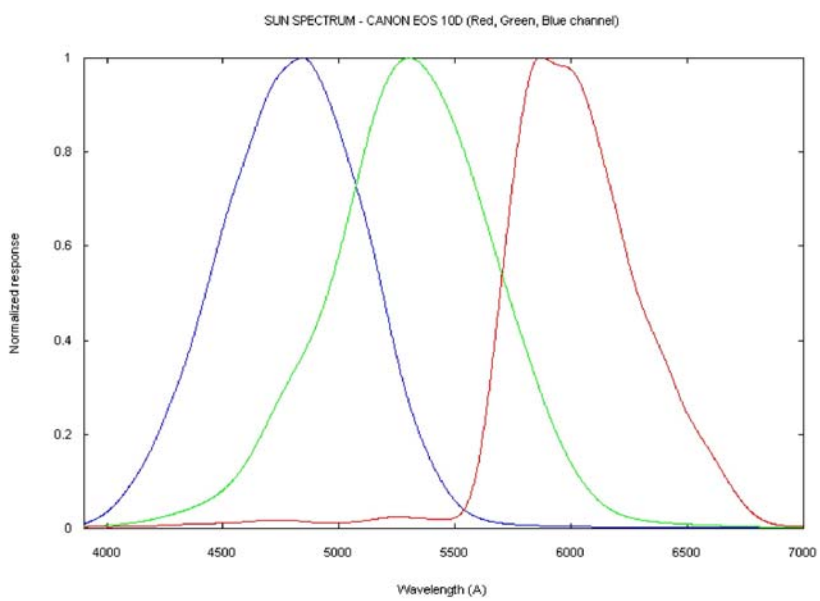

Figure 2.3: Buil (2004b) has obtained relative transmission curves for the RGB filters.

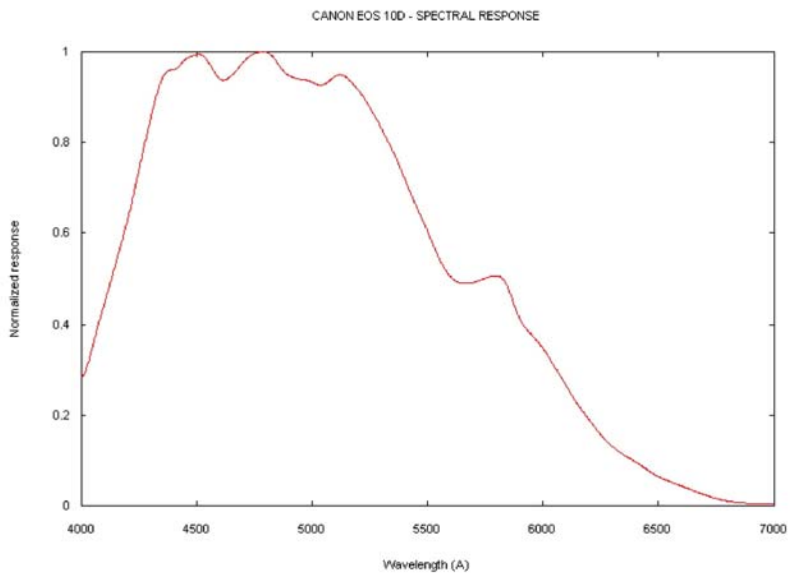

Figure 2.4: A relative overall quantum efficiency plot from Buil (2004b).

2.6. Read-Out Noise and Gain

The read-out noise and gain of the Canon EOS cameras and of the Nikon D70 CCD-based DSLR have been measured by Buil (2004b), by Lovejoy (2004a); Lovejoy (2004b) has further tested the more expensive Canon 1D Mk.II. Their results are thoroughly professional and highly consistent. Table 2.1 is a summary of their combined results, to which I have added numbers from the datasheet of the Electrim EDC-3000D monochrome camera (see below). The Nikon D70 is included for comparison with a high-end CCD based camera.

The DSLR cameras have various gain settings, identified by ISO numbers by analogy with film. Most commonly with the Canon DSLR's, ASA 400 is used.

Table 2.1: Characteristics of discussed detectors

Chip	Format NX × NY	Pixel size μm	Typical gain e-/ADU	Readout noise (e-)	Dark e-/s/pix	Temp (C)
10D/300D	3072 2048	7.4	2.41	15	1	22
20D	3504 2336	6.6	3.14	7.5	0.5	22
1D-II	3504 2336	8.2	2.51	7.0	0.3	22
D70 CCD	3040 2014	7.8	2.98	19.0	24	22
EDC-3000D	1280 1024	5.2	...	10	20	25
IBIS4-14000	4560 3048	8.0	...	35	220	22

Table 2.1 shows that the readout noise of the best DSLR cameras is now as good as or below that of the commonly available Thermo-Electrically cooled CCD cameras (SBIG, Apogee, FLI etc.), but somewhat higher than the 5 electrons typical of "science grade" cryogenically-cooled CCD cameras. However, the smaller pixels and Bayer color matrix reduces their quantum efficiency compared with monochromatic full-frame CCD's.

2.7. Dark Current

In the un-cooled BRITE environment, we can expect 10 – 20 C as a typical working temperature. With older-style CMOS detectors, dark currents of 1000 e-/sec/pixel at 20 C are not uncommon, which severely restricts the usefulness of such devices. However, the work of Buil and Lovejoy, quantifying what dozens of amateurs have found qualitatively (see the "digital_astro" Yahoo group, for example), proves that the Canon CMOS cameras have extremely low dark current at room temperature. In fact, Lovejoy has posted usable exposures as long as 28 minutes at 10 C. The dark current rate of 1~e-/sec/pixel at room temperature is less than that of the dark current of the Kodak KAF series CCDs (1 e-/sec/pixel at 0 C), which are themselves very good. The evidence is that Canon have reduced the dark current of CMOS detectors to below that of CCD's.

In Figure 2.5, I have computed the dark current per pixel using equations 7.44 and 7.46 of Janesick (2001), with a figure-of-merit dark current of 1 pA cm^2 at 300 K. This is at the very lowest value expected for CCD's. Furthermore, the Canon chips are extremely clean, with few hot pixels. This is seen clearly in Figure 2.6 from one of Buil's comparison of the 10D with the Nikon D70 CCD-based camera.

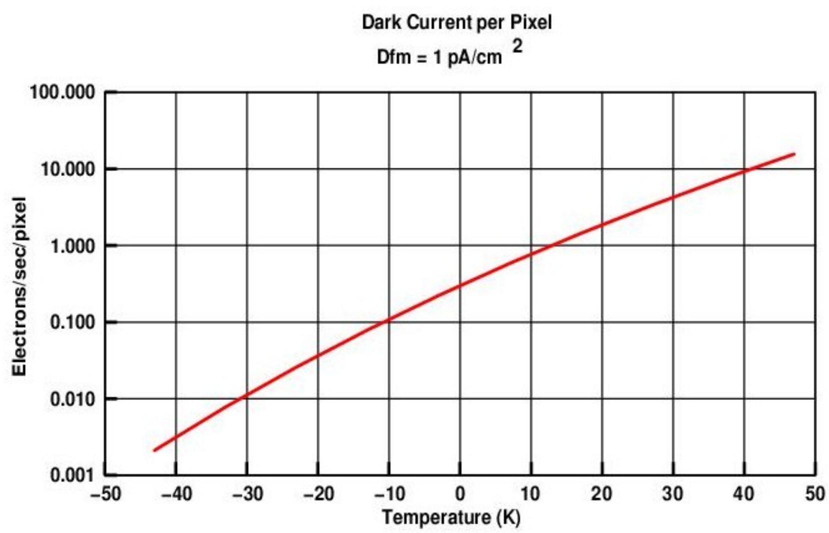

Figure 2.5: Dark current from Janesick's Formula.

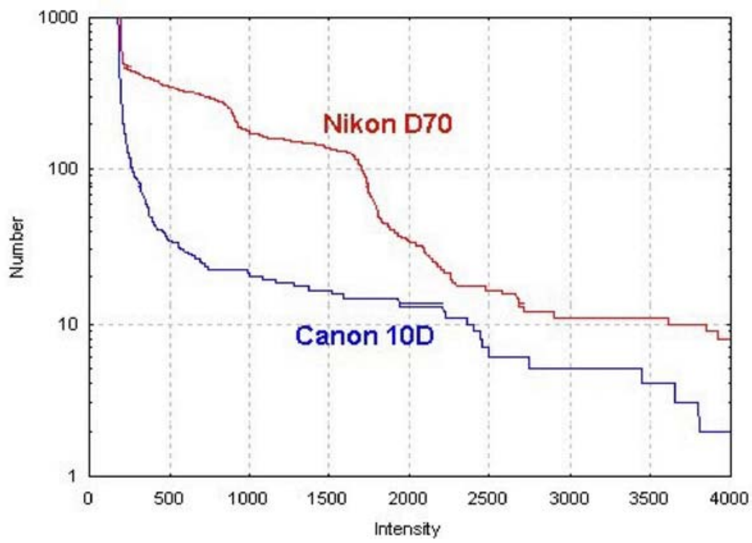

Figure 2.6, reproduced from Buil 2004a. Inverse cumulative histogram of the thermal signal (from RAW data). Dark exposure of 120 seconds with ISO 400 and 21 C. Note that the vertical scale is logarithmic. In the Canon 10D image there are 20 hot pixels which have an intensity higher than 1000 ADU. For the same exposure time, in the case of the Nikon D70 there are 200 pixels which have an intensity higher than 1000 ADU (mode 3). Before correction, the dark signal of the D70 is typically 10 times higher than that of the 10D. In both cases several families of hot pixels are identified.

2.8. Small scientific CMOS cameras

I searched the Web for other new CMOS cameras, and found a number of compact cameras in the 1 – 2 Mpixel range, by such manufacturers as Altasens, Electrim, Basler and Aries. Only the new Electrim EDC-3000D monochromatic camera is relevant. It is a 1.3 Mpixel CMOS camera, with 5.2 micron pixels (rather small), progressive scan, full-well capacity 40 Ke-, dark current 20 e-/sec/pixel (very good), quantum efficiency 56%, exposure time 8 μsec to 10 sec, 10 bits ADC, readout noise 10 e- (very good). It can read out at 30 full frames per second, or up to 100 frames per second over a selected smaller region of interest. The entire camera in its container weighs 145g, with all power supplied from the USB 2.0 bus, and costs less than US$1000. This is an interesting camera, but its pixels are rather small, and it has only 10 bit digitization. If the other electronics are efficient, the whole camera could be suitable for BRITE. Electrim has a long history of supplying scientific CCD cameras.

2.9. Large scientific CMOS cameras

A large chip can allow us to access the originally desired 30-degree field. Of special interest are chips with well over 10 megapixels. Such a sensor is the Fill Factory IBIS4-14000-M (3048 × 4560, 8μm pixels, 3 Hz max full-frame rate). According to Meynants et al. (2004), their simple "3-transistor active pixel" has the advantages of a larger full-well capacity, a higher fill factor (eliminating the need for microlenses) and lower cost, at the expense of 10-times or higher dark current. However, we do have verbal indications of a lower dark current (40 electrons/sec, rather than 220 at room temperature). This chip has the full 35mm format (36 × 24 mm), which at f/2.2 would provide us with a field of 38 degrees on the long axis, at 30 arc seconds per pixel.

2.10. Performance simulations

I have developed a spreadsheet to very crudely model the imaging by BRITE. I compute the signal-to-noise of a star spread over an aperture of 2 arcminutes diameter, integrated over an aperture of 2 arcmin radius. I assume a telescope aperture of 25 mm. I compare a Canon 10D/300D type of chip with the Electrim EDC-3000D detector. The calculation is completely standard, including source photon noise, readout noise, sky background photon noise, dark current quantum noise, optical efficiency factors, quantum efficiency. At this stage I am not considering digitization limits, saturation or flattening limitations.

The observing strategy with multi-megapixel detectors with limited dynamic range is to spread the stellar images over a fairly large number of pixels. I am assuming a 2 arcmin software extraction aperture. Given that the diffraction limit of a one-inch telescope is 5 arcsec, this requires appreciable apodization[2]. We need to determine what the maximum integrating aperture size can be to avoid source confusion (contamination by other stars).

A large point-spread function with unmodified Bayer matrix colour sensors makes sense, since the over-sampling reduces the errors due to the geometrical mismatch of the three colour channels. There may be benefit in having three-passband measurements, but there is a serious penalty due to the rejection of light by filters of relatively narrow passband.

Optically, the Electrim chip allows a 12.7 degree extent along the longer axis of the chip at f/1.2 (41"/pixel), whereas the bigger Canon 10D/300D chip covers 35 degrees along the longer axis at f/1.5 (36"/pixel). The calculation is presented in Figure 2.7. The lower S/N of the Canon chip is due to the lower effective quantum efficiency due to the Bayer matrix filtering.

The IBIS4-14000 chip provides very good performance, with a much larger size permitting a more relaxed f/ratio of 2.2. It also has a larger full-well capacity, at 65,000 electrons, than the Canon pinned-diode design.

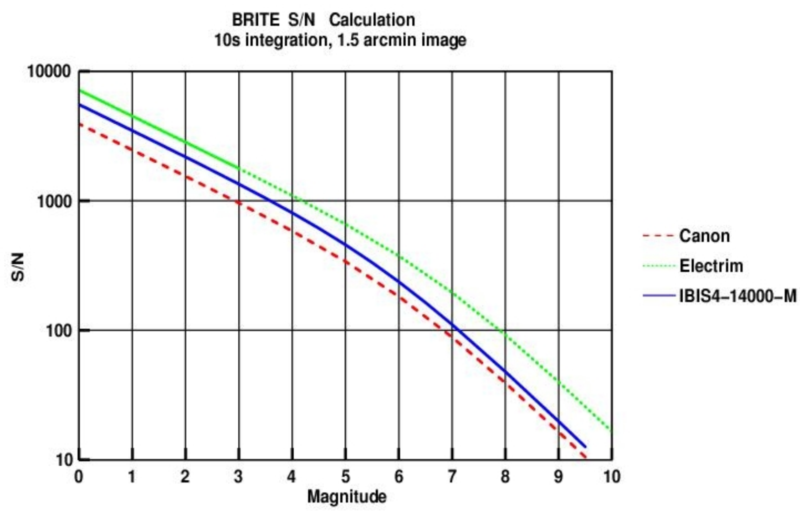

Figure 2.7: Signal to noise ratios for 10 second BRITE integrations

[2] The term “apodization” refers to removal of high spatial frequencies from the point spread function.

2.11. Further requirements

What these preliminary results show is that the best CMOS detectors are fully capable of supporting the BRITE mission. Since their technology is rapidly evolving, the final design must address the matter of the most appropriate form, with sufficiently low power consumption.

It would be highly desirable to obtain stand-alone Canon CMOS detectors WITHOUT Bayer matrix filters. An approach to Canon may be highly desirable. It may be possible to gut a standard Canon digital camera of unneeded hardware, but clearly Canon's involvement or assistance would be most desirable. The Canon chips would give us the desired field of view, at a more relaxed f/1.5.

The Electrim camera would also work well, as is if the power requirements are low enough, though its field of view is not as good as the Canon chips allow. Its dark current is essentially negligible for our purposes, despite being 20 times higher than the Canons; this shows just how good the Canon chips are.

The most encouraging approach now is definitely the Fill Factory IBIS4-14000. With its lower dark current, and promise of even lower values, it is much better than the previous Fill Factory chips. Furthermore, with its lack of colour filters, analog output and higher quantum efficiency, without microlenses, it offers advantages over the other chips I have discussed. Above all, its large format gives us the full 30 degree field (38 degrees along the longer dimension), at f/2.2.

It is essential that scattered light be eliminated. I would propose sacrificing some optical transmission efficiency to have a low-scattering optical design.

2.12. Conclusions

I have shown that measurements by expert amateurs indicate that the best large CMOS detectors are extremely effective, and that the performance of CMOS detectors is not a limitation. In fact, BRITE could be a more general-purpose photometric instrument than had been assumed, since it could get 1% photometry in 10 seconds down to 8th magnitude.

3. ORGANIZATION DETAILS OF THIS STUDY

The study was conducted in parallel by two sub-teams: The CMOS detector study was done by the University of Toronto (Department of Astronomy and UTIAS/SFL) and Dynacon group while the optical study was done separately by Ceravolo Optical Systems. A one-day meeting took place at David Dunlap Observatory of the whole Concept Study team on February 18, 2005, where details of the preliminary optical design were discussed, in relation to what was known about the CMOS detectors at that time. All remaining contacts of the UofT and Ceravolo groups were over e-mail & phone. The UofT and the UTIAS groups worked very closely in locations and met several times.

The CMOS detectors were tested for angular sensitivity variations at the David Dunlap Observatory using various optical elements available there. Additional components were an optical fiber-based point-source and various cables and adapters needed for transferring images between cameras and computers and for permitting long exposure times. The thermal tests of the detectors were done using the thermal chamber of UTIAS/SFL. Finally, images of the sky were taken at DDO with one of the cameras (Canon) by attaching it to the 1.88m telescope.

Following the recommendations in Section 2, we initially selected 3 detectors for the study: (1) Digital Rebel Canon 300D, (2) Electrim EDC-3000D and (3) FillFactory IBIS4-14000, each costing slightly over $1000. Camera (1), sold with a zoom lens, is an off-the-shelf item which we purchased with a fixed focus 50mm f/1.8 lens for sky-imaging tests. Obtaining camera (2) took us almost two months resulting in delays; we could test it last in the study. The camera was sent set to 8 bit/ADU digitization; achieving its 10 bit/ADU capacity required many contacts with the manufacturers and some modifications of the camera software and hardware. The biggest disappointment was the high cost of the IBIS4-14000 development kit, initially quoted at about $1000, but with the final price of US$5,000. We could not afford this and thus limited the study to the first two detectors. In retrospect, analysis of 3 detectors would not be feasible within the allotted time, particularly because of the very slow rate of measurements in the thermal chamber. As we understand, Dynacon Inc. has ordered the IBIS4-14000 development kit for their own tests; the expected delivery date will be several weeks after the end of this study.

The assumed field of view of BRITE was 25 degree diameter. If sampled at a scale of 0.5 arcmin/pixel, this would require a 3600 × 3600 pixel detector. This would be almost satisfied by the Canon (3072 × 2048 pixels) or the IBIS4-14000 camera (4560 × 3048), but definitely not by the Electrim (1280 × 1024 pixels); the latter was selected for its other advantages, as an example of a scientific CMOS camera.

The exceptionally low level, practically the absence, of any thermal (“dark current”) signal in the Canon detector forced us to consider a possibility that the thermal current is evaluated and subtracted in the camera in real time. Thus, the thermal signal build-up for this detector was estimated indirectly from the thermal noise.

The optical preliminary design was driven primarily by (1) avoidance of vignetting, (2) angular limitations on the incident beam set by CMOS detectors (necessity to have light rays to strike the detector at closest to the right angle and the f/ratio not too small) and (3) sufficient sampling of the images for all positions on the detector with the assumed “speed” of the system of f/2.0. The overall size of the lens system of 100mm and the focal length of 70mm were the initial assumptions.

4. ANGULAR SENSITIVITY DEPENDENCE TESTS

4.1. Experimental setup

The experimental setup used to determine the angular dependence of the imagers tested is shown in Figures 4.1. and 4.2. The imager under test is mounted on a single-axis rotary stage which allows for a full 360 deg of rotation, and which has a vernier drive with 4 arcmin markings. Between the imager and the rotary stage is a small translation stage which is used to align the imager’s centre with the centre of rotation.. This entire assembly is mounted on a jack, which allows for adjusting the elevation of the imager with respect to the rest of the apparatus.

The remaining equipment is mounted on a small optical rail. A fibre-optic light source, of the kind used to collimate small telescopes (“PicoStar” Artificial-Star Collimator) is used to provide illumination of the imager. The source is mounted on a small transverse translation stage, which allows for aligning the source with the axis of the optical bench. The source produces a mildly divergent beam, which is focused on the imager by a small achromatic lens of approximately 175 mm focal length, installed on a mounting post on the optical bench. The height and rotation of the lens is adjustable to produce the desired image on the imager.

The entire assembly is installed inside a large wooden frame, on which is draped a heavy black drop-cloth. This is used to prevent stray light from reaching the imager. In addition, the windows of the lab are also covered in the same drop cloth, preventing outside light from reaching the imager. Ancillary support equipment is provided outside of the light-blocking enclosure: a power supply for the light source, another supply for the imagers, and a laptop computer for storing the images. Finally, a number of small shims and angle brackets are used to orient the imager whenever the plane of rotation needs to be changed.

4.2. Experimental method

4.2.1 Setup and alignment

The imager under test is mounted on the translation stage attached to the rotary stage. If necessary, a right-angle bracket is used to alter the rotation axis of the imager.
The entire apparatus is then roughly aligned by eye:
1) the imager normal is aligned with the optical bench
2) the height of the source is aligned with the height of the imager
3) the source is aligned so that its beam is roughly collinear with the optical bench

Following this, the imager normal is aligned with the optical bench as follows:
1) a lens is installed on the imager, and the rotary stage is rotated until the image of the source is visible near the centre of the image
2) the lens is removed, and the bench-mounted achromatic lens is installed
3) the rotary stage is rotated until the image is reasonably close to where it was with the imager-mounted lens

4) steps (1) through (3) are repeated iteratively until there is little motion of the source image; the criterion used is 100 pixels of motion.
5) the transverse position of the source is adjusted until the image is in the middle of the imager.

After alignment, the coincidence of the imager plane and the axis of rotation is checked:
1) the bench-mounted achromatic lens is installed, and its position adjusted until the source is focused
2) images of the light source are taken with the rotary stage at +40 deg and -40 deg.
3) if the image location changes by more than 20 pixels, the translation stage on which the imager is mounted is adjusted, and the process is repeated.

Following this, a check is performed to determine if the rotation is only in one plane:
1) the bench-mounted achromatic lens is removed, and a lens is mounted on the imager
2) the rotary stage is adjusted until the image travels almost to one side of the sensor, and an image is taken
3) the rotary stage is adjusted until the image travels almost to the other side of the imager, and an image is taken
4) if the image wanders by more than 2% vertically, the rotary stage is shimmed appropriately, and the alignment process is repeated.

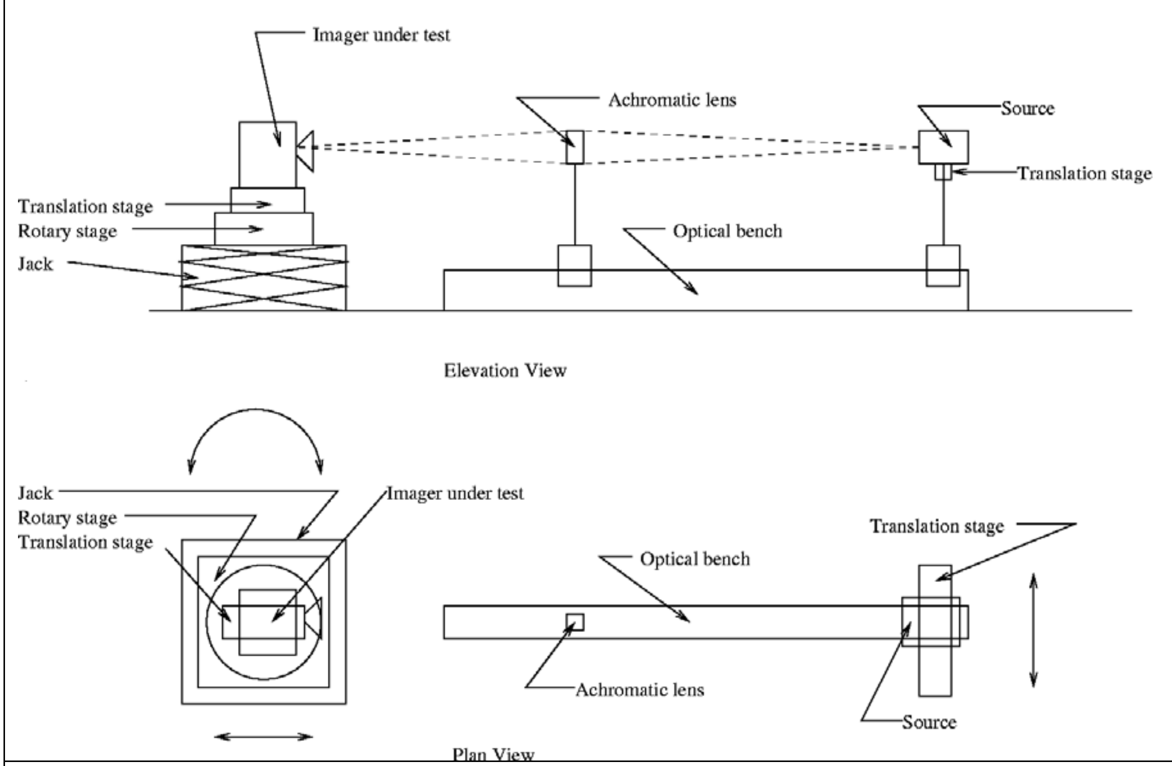

Figure 4.1: Experimental setup

Figure 4.2: Experimental setup

Finally, the source level is set:
1) the bench-mounted achromatic lens is adjusted to produce an image of about 30 pixels in diameter;
2) an image is taken, and the maximum pixel value is recorded;
3) both the exposure time and the source intensity are adjusted to drive the maximum pixel value to the midpoint (2048 ADUs for Canon, 128 ADU for Electrim);
4) steps 2 and 3 are repeated until a reasonably short exposure (less than 1 second) is required to produce mid-level outputs.

At this point, the equipment is ready for experiments.

4.3. Experiments

Two sets of experiments are run for each imager: one to measure dependence on the imager "yaw" angle, and one to measure the dependence on the "pitch" angle. The latter is accomplished by mounting the imager on a custom right-angle bracket. The yaw axis is defined as being the "vertical" axis of the camera: When the camera is held in its usual configuration (flash facing upwards; tripod mount facing down), then a yaw rotation is the equivalent of panning horizontally. Similarly, the "pitch" axis is the horizontal axis running from the left to the right edge of the camera. A pitch motion is equivalent to panning the camera up or down.

Before each set of experiments, the imager is aligned as described above. Then, with the apparatus enclosed in the baffle box, and with the lab lights turned off, ten images are taken at each angle (pitch or yaw) between +40 and -40 degrees, inclusive. The resulting images are recorded on an attached laptop computer in "raw" format; that is, with no post-processing by the camera. As a result, pixels are uncorrected and uncompressed, and the full resolution of the pixel analogue-to-digital converter is maintained.

For each imager, a constant exposure time is used. For the Canon imager the exposure used is 0.6 seconds. All relevant data about the exposure levels is also stored with the associated image in "Exif" format.

4.4. Data reduction

The data reduction process uses two pieces of software for the canon camera and only one for Electrim. The first is IRIS[3] version 3.43. This program is used to import the raw files from the Canon imager, to separate Bayer-matrix-filtered images into their constituent planes if required, and to remove bias.

The second program used for both cameras is the PyFITS package[4], version 0.9.3. This, combined with a short script (included as Appendix 4.A.1), is used to reduce the bias-corrected, plane-separated images into an angular response. A simple algorithm is used, which simply integrates the intensity over a selected region of the image.

The data reduction procedure is as follows (steps 1-3 only for Canon):

---

[3] IRIS is a image processing package distributed by http://www.astrosurf.org/buil/us/iris/iris.htm

[4] PyFITS: http://www.stsci.edu/resources/software_hardware/pyfits/

1) in IRIS, import all of the images for a particular rotation axis by using the “Digital photo/Decode RAW Files...” menu option
2) in IRIS, convert the imported RAW files to colour images by using the “Digital photo/Sequence CFA conversion...” menu option
3) in IRIS, a manual RGB separation is performed, due to a bug which prevents the automatic separation from being performed. The following steps are performed, in sequence, once per CFA image:
    3a) the CFA image is loaded using the LOAD command
    3b) the CFA image is converted to an RGB image using the CFA2RGB command
    3c) the RGB image is separated into planes using the SAVE_TR command
4) for each angle, a bounding box is determined, over which intensity will be integrated:
    4a) a representative image for each angle is opened. The choice of which image in sequence is chosen, as well as which plane is used, is not important, as the planes are coincident, and the image does not wander between successive exposures at a fixed angle.
    4b) a bounding box which enclosed the image and some surrounding background is picked, and its dimensions noted
    4c) after all angles are processed, the largest bounding box necessary is selected, and the process is repeated until all images fit within a bounding box of a constant size.
5) the intensity is integrated over the bounding box for all the images.

4.5. Results Canon

The numerical data are given in tabular form in Appendix 4.A.2 to this section. The integrated intensities, normalized arbitrarily to the maximum of the green channel are shown in Figures 3.3 & 3.4. As can be seen, the red plane has the lowest absolute response, though its relative response generally follows the shape of the other two (blue and green) channels.

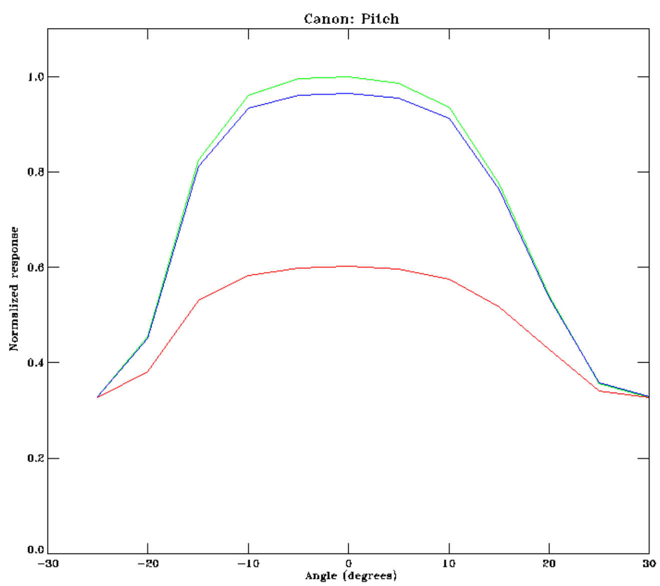

Figure 4.3: The relative responses for the Canon camera, normalized to the maximum of the green channel, for the “pitch” rotation. The coloured curves correspond to the channels: green for G, blue for B and red for R. The angular dependence is moderately flat to ±15 degrees, and it drops abruptly. The formal *rms* errors are too small for being shown; besides the accuracy is limited by systematic errors which are difficult to quantify.

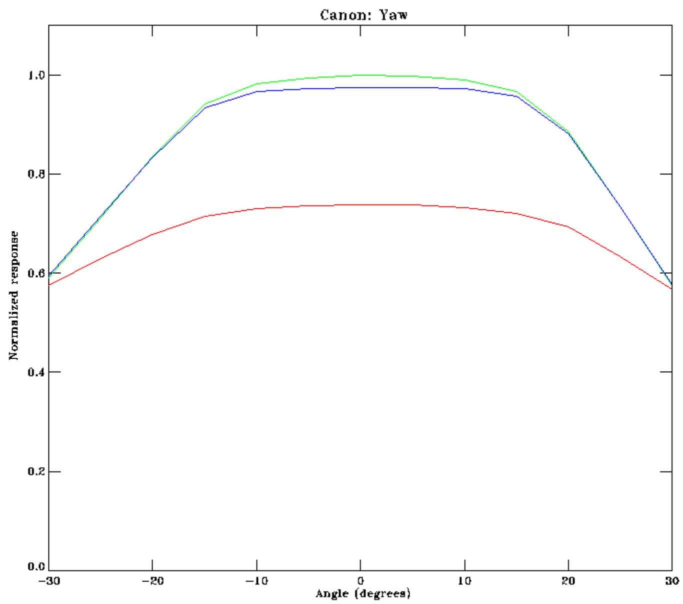

Figure 4.4: The relative responses for the Canon camera, normalized to the maximum of the green channel, for the “yaw” rotation. Note that rotation around this axis produces a different picture than for the “pitch” rotation.

At extreme angles, the imager sensor can become obstructed by the camera body; this results in portions of the image being cut off. Figure 4.5 shows an example of this effect. As a result, the integrated response becomes smaller than it would otherwise be, if the obstruction did not happen. For the Canon imager, obstructions were first observed at yaw angles of -30 and +25 degrees, and at pitch angles of -20 and +20 degrees.

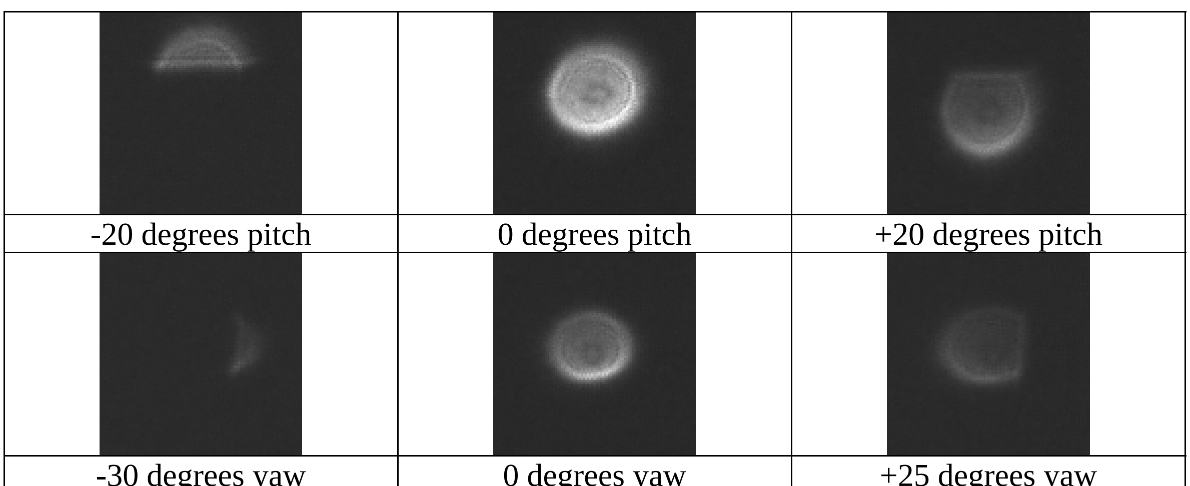

Figure 4.5: Image obstruction in Canon imager

The curved maximum of the Canon CMOS sensitivity curve can be characterized by the decrease in sensitivity at a fixed distance from the axis. In Table 4.1 below we give values of the percentage sensitivity drop at ± 12 degrees from the perpendicular to the detector. At this time it is unclear if small asymmetries in these data reflect the real asymmetries in the pixel illumination or have resulted from imperfections in our measurements. Certainly, the large difference in the pitch and yaw dependencies must be due to geometry of the pixel illumination. The value of ± 12 degrees was selected in relation to the current plans concerning the choice of the BRITE field.

Table 4.1: Canon camera. Decrease in sensitivity at ± 12 degrees

Rotation	Colour channel	% drop left or down	% drop right or up
Pitch	Blue	-16	-22
	Red	-12	-14
	Green	-17	-22
Yaw	Blue	-4	-3
	Red	-3	-3
	Green	-6	-3

4.6. Results Electrim

The angular dependence of the sensitivity on the incidence angle is shown for the Electrim camera in Figure 4.6. Results for both angles are shown on the same plot. The numerical data are given in the Appending 4.A.3.

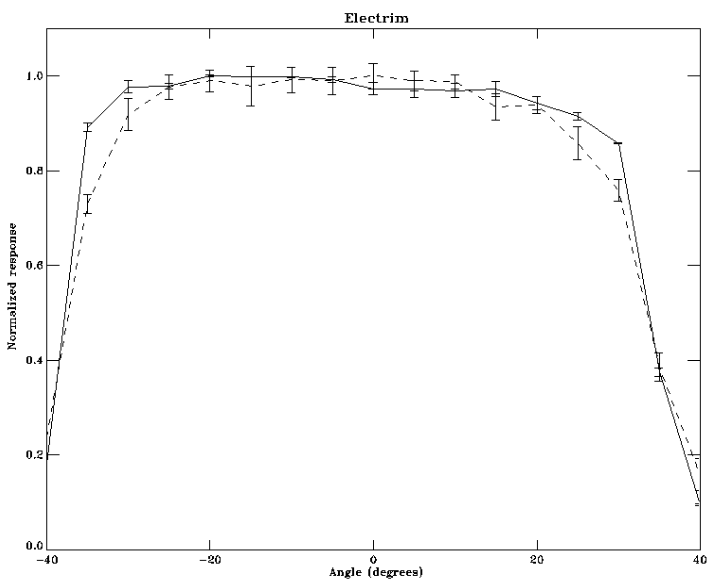

Figure 4.6: The angular dependence of the sensitivity on the “pitch” (broken line) and “yaw” angle (solid line) for the Electrim camera. Note the random errors are larger than for the canon camera, partly because of the sampling errors at 8 bit/ADU. Note also that the range in angle is larger, ± 40 degrees rather than ± 30 degrees.

The Electrim camera shows a flat response in both angles, a picture very different from that for the Canon. The numbers characterizing the drop in sensitivity at 12 degrees from the optical axis (as in Table 4.1) are: pitch -3% and -6%, yaw 0% and -3%, with the error for each at the level of ±2%. We have been informed by the manufacturers of the Electrim camera that their detector has micro-lenses (no similar information can be obtained for the highly proprietary product of Canon), so either the lenses are of better quality than in the Canon camera, or the chromatic effects are absent or manufacturing specifications of different level of stringency. Small asymmetries in the response may be due to difficulties we experienced with our measuring system to insure the exact perpendicular position of the detector to the light beam at the nominal angle of zero degree incidence.

The Electrim camera body intercepted part of the beam much larger angle that for the Canon camera. For pitch, at +35 degrees, the beam is partially obstructed, +40 is entirely blocked, -35 is partially obstructed, and a small amount of light is visible at –40 degrees. For yaw: +35 is partially obstructed, +40 is entirely blocked, -35 is partially obstructed, and a small amount of light is visible at –40 degrees.

4.7. Conclusions

The two cameras show very different behaviour in terms of the angular dependence of the sensitivity. The Canon camera shows a curved dependence within ±12 degrees and a very rapid drop-off in the sensitivity beyond that so that the FOV would be limited to < 25 degrees in diameter. In contrast, the Electrim camera has a flat response within a wide range of angles to ± 30 degrees. For angles corresponding to the planned size of the BRITE field (± 12 degrees), the Canon camera shows a drop in sensitivity of about 15% – 20% in the pitch angle and 5% in the yaw angle, whereas the Electrim camera shows a drop of only about 3% in both rotations.

These differences demonstrate very well the range of situations which can be encountered in the final selection of the detector for BRITE.

Appendix 4.A.1: Data-reduction script

The following script is written in Python, and requires the use of PyFITS and numarray.

```
"""Usage: angle.py x1 y1 x2 y2 files"""

import sys
from numarray import ravel, sum, Int64
import pyfits

x1 = int(sys.argv[1])
y1 = int(sys.argv[2])
x2 = int(sys.argv[3])
y2 = int(sys.argv[4])

for fn in sys.argv[5:]:
    print fn,
    ffile = pyfits.open(fn)
    data = ffile[0].data.astype(Int64)[y1:y2,x1:x2]
    inten = sum(ravel(data))
    print inten
```

Appendix 4.A.2a: Raw results: Canon imager, pitch plane

	Blue		Green		Red	
Theta	Mean integrated intensity	Standard deviation	Mean integrated intensity	Standard deviation	Mean integrated intensity	Standard deviation
-25	1308872.7	6711.82	1303416.2	5398.87	1297840.1	5253.82
-20	1789640.4	5709.2	1803441.7	3716.71	1514432.1	5532.34
-15	3222672	6935.49	3275104.8	4828.5	2106816.8	6201.88
-10	3706319.8	6582.13	3808445.2	3941.52	2310187.4	4674.47
-5	3808986.1	6277.86	3948100.2	3431.56	2377027.2	5490.57
0	3829517.7	4515.61	3966183.5	5293.08	2389699.9	4215.71
5	3787558.8	2824.16	3913514.1	4033.97	2368883.8	6386.63
10	3623547.6	5492.8	3709092.3	3716.19	2284738.7	5904.84
15	3029719.8	5879.24	3075796.2	5130.87	2050537.9	5601.32
20	2126505	3933.71	2140477.3	4063.21	1699217.8	6588.42
25	1423300.9	6218.55	1413714.8	4743.52	1351494.6	4919.77
30	1305436.2	4975.66	1300574.4	4590.15	1294490.7	6665.78

Appendix 4.A.2.b: Raw results: Canon imager, yaw plane

	Blue		Green		Red	
Theta	Mean integrated intensity	Standard deviation	Mean integrated intensity	Standard deviation	Mean integrated intensity	Standard deviation
-40	1308640.2	6029.34	1303310	3360.48	1297434.1	4827.33
-35	1309021.2	7850.57	1302877	4766.57	1296510.9	3547.86
-30	1372354.3	6119.25	1363516.2	4028.72	1329432.9	3168.99
-25	1650019.4	6852.47	1641106	4782.36	1452818.8	5171.85
-20	1922630	4308.37	1925910.6	3732.22	1565104.9	4726.57
-15	2156981.4	6124.8	2173693.4	3058.98	1649039.9	3899.26
-10	2230773.9	5106.43	2267239.9	3358.43	1683882.7	3188.53
-5	2242961.7	5282.58	2294232.6	4520.66	1697299.6	6249.49
0	2251623.3	7951.87	2307826.4	4604.76	1702693.5	3967.44
5	2249409.9	5298.12	2304417.7	4080.15	1701516.3	5912.82
10	2243942.8	5899.48	2287348.5	3288.72	1689965.7	5232.72
15	2207006.6	6027.74	2232516.5	5007.35	1665007.6	6092.79
20	2033626.6	4904.53	2044388.7	3411.72	1600052.4	7557.79
25	1695727.5	7066.55	1694456.2	4631.13	1464134.6	4202.69
30	1332281.3	6237.43	1329165.5	5140.12	1309894.8	5497.17
35	1307951.8	5155.04	1302081.8	4401.39	1295331.3	5885.39
40	1308979.8	3849.66	1301843	2925.89	1295218.8	4891.84

Appendix 4.A.3: Raw results: Electrim imager

Theta	Pitch	Std dev	Yaw	Stddev
-40	36199	4737	24114	133
-35	112271	3058	119006	1224
-30	141626	5211	130441	1652
-25	150253	4000	130497	798
-20	152433	3496	133502	196
-15	150662	6577	133258	97
-10	152706	4108	133227	131
-5	152371	4517	132468	768
0	153992	4098	129948	1776
5	152455	3238	129771	2372
10	152078	2218	129402	1930
15	143971	4229	129767	2091
20	144534	2764	125892	1879
25	132012	5341	122142	991
30	116745	3450	114507	83
35	59282	4571	49996	1153
40	24417	5162	12689	177

5. THERMAL NOISE

5.1. Introduction

Digital noise originates from a variety of sources and thus can be classified into these classes:

i) Readout noise: Arises due to errors in reading the signal in the amplifier circuit. The magnitude of this noise is usually constant, however it is random in nature.
ii) Thermal noise, which is also called dark current noise. This noise is attributed to molecular agitation and thus depends on the temperature of the detector.
iii) Discrete quantization: Arises in the conversion of the analog signal to a digital format.
iv) Bias: An electric offset which may vary between pixels. This results in a repeatable pattern that can be subtracted from every science frame. It is an additive effect.
v) Sensitivity variations: Each pixel in the detector array has a slightly different sensitivity to light. It is a multiplicative effect which can be corrected by taking “flat images” at the cost of increased random noise.

This study addresses the random components of the noise, items i) and ii). To quantify these noises, dark frames and bias frames were acquired at various temperatures. With these images the dark current, read-out noise, and the bias frame can be determined. In order to express these values in terms of electronic noise rather than in ADU units, one must determine the electronic gain for the cameras.

The dark current signal is of crucial importance for the BRITE application as it accumulates over time in long exposures. The surprisingly low values of the dark signal obtained by advanced amateurs for the Canon camera (and confirmed by our experiments) forced us to consider a possibility that the *dark current signal is actually subtracted in these cameras in real-time* and does not directly show in the images. However, the increased noise will appear even if such subtraction is done. Hence, our approach was an estimation of the dark signal through measurements of the noise rather than of the signal itself. This assumption turned out to be a correct one: The noise increases with time, as expected; the details will be described in Section 5.3 and following.

5.2. Test Setup

5.2.1. Dark and Bias Setup

In order to determine the dark current and the bias pattern of the camera, a series of dark and bias frames were captured at various temperatures. Dark current, or thermal noise, is a function of temperature and thus was tested throughout the expected operating range of a spacecraft, which is roughly -20^{o}C to +30^{o}C. In order to ensure the detector captured no stray light, the camera was placed in a sealed thermal chamber with the camera lens cap on. Furthermore, since stray light can enter through the viewfinder, this was also covered. It should also be noted that during operation, the temperature of the detector rises due to thermal dissipation. Considering that thermal noise is a function of temperature, this was accounted for as much as possible by allowing the camera to cool down to the ambient steady environment after every exposure. A profile of temperature vs. time for one of the tested temperature settings (+10^{o}C) is shown in Figure 5.1.Temperature sensors were mounted in three locations on the camera. No temperature sensor could be placed near the detector itself as this would force the removal of the lens cap which was required to be in place to eliminate stray light from images. The complete test setup in itemized form is listed below. Note that the test setup is described with the sepcific reference to the Canon camera; however, the dark current and bias tests of the Electrim camera were very similar. Pictures of the test setup are shown in Figures 5.2 a) to d).

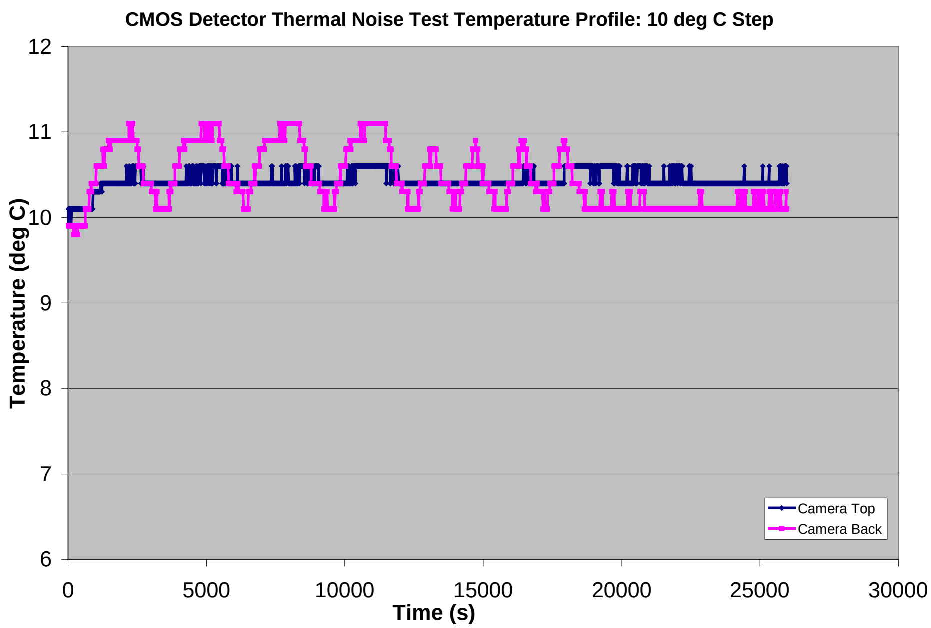

Figure 5.1: Thermal noise testing temperature profile for the Canon camera. Large fluctuations in temperature with peak-to-peak amplitude reaching one degree occur due to camera operation. Note temperature stabilized to a steady state prior to subsequent image capture.

5.2.2. Dark Frame and Bias Frame Test Setup:

1) Ensure thermal chamber is light tight. Seal any locations where light can possibly enter.
2) Attach temperature sensors to camera at various positions so that operating temperature can be recorded.
3) Setup camera in the thermal chamber: Ensure LED's do not activate when capturing image. Place lens cap on camera. Block viewfinder of camera to prevent any possible stray light from striking detector.
4) Visually ensure that the thermal chamber is sealed. Take pictures inside the thermal chamber in a brightly lit area to confirm that no stray light is entering.
5) Capture images with camera at 10 degree steps from –20^{o}C to +30^{o}C (6 steps)
   - Take exposures of 1/4000 (bias), 1 and 10 seconds, 1, 10 and 30 minutes[5].
   - For each exposure length, take images at camera ISO (detector sensitivity) settings of 100 and 400 (Canon).

[5] The longest exposure with the Canon camera is 1 sec so that a special (in house built) circuit and software were used for long exposures. The Electrim camera has a limit of 10 sec which could not be changed.

- Take two images per setting (ISO and exposure length) for images greater than and equal to 1 minute in exposure length. Take five images per setting for all images less than 1 minute in exposure length.
- For each image record the operating temperature and time of image.

6). Convert each RAW image to a .FITS format for subsequent data reduction.

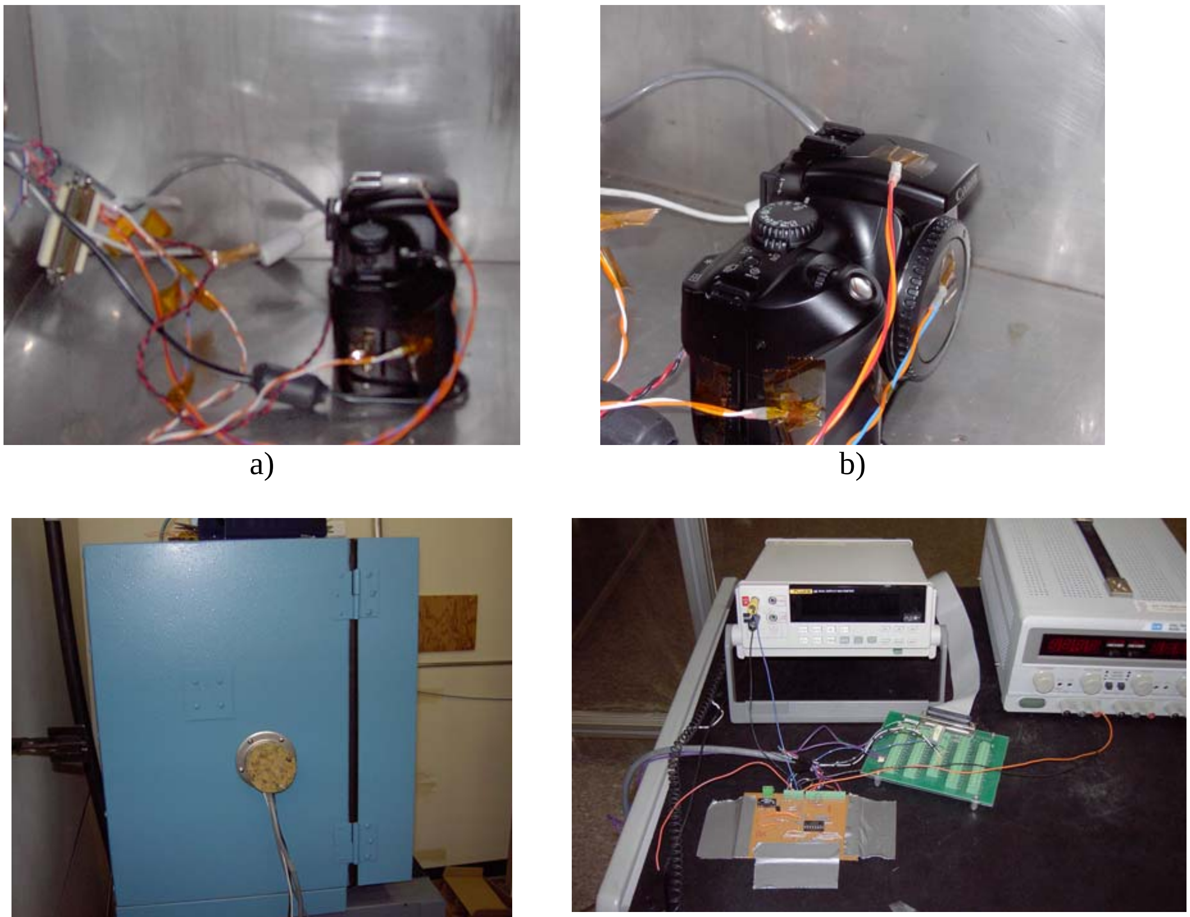

a) b) c) d)

Figure 5.2: CMOS detector thermal noise test setup. a,b) The Canon camera and wiring arrangement in thermal chamber. c) Sealed thermal chamber. d) Temperature readout electronics.

5.2.3. Electronic Gain Setup

The signal generated by the interaction between incident photons from the scene and the detector itself is converted into a digital form. Depending on the amount of bits used to convert the signal from each pixel, the intensity of the signal is subdivided into a discrete number of intervals called Analog to Digital Units (ADU). The Canon 300D encodes the signal into 12 bits, and therefore will convert the signal into a quantized signal of up to 2^{12} or 4096 discrete intervals of intensity.

The Electrim camera utilizing a Micron CMOS detector was sold to us on condition that it can be switched between 8-bit and 10-bit modes, the latter just marginally useful for the same level of precision as we have reached for the Canon camera. Unfortunately, in spite of a lot of effort on our part and many contacts with the manufacturers, we have not been able to use it at 10 bits because the provided (third party) software was simply inadequate. The limitation to 8 bit/ADU was not crucial for the angular sensitivity measurements reported in Section 4, but prevented us to do meaningful tests of the thermal properties of the Electrim camera. With the very crude 8-bit sampling, we could only determine the gain for this camera, but were not able to say much about the thermal noise properties. We can only state that the dark current was miniscule compared with the readout noise for exposure times shorter than 1 sec.

The electronic gain of the camera, measured in electrons per ADU may be taken as a measure of the camera sensitivity, specifically the number of electrons that are required to register a single brightness step (ADU) in each pixel of an image. Photographers use a scale of ISO or ASA units with larger numbers representing higher sensitivities. For convenience of the customers, manufacturers of cameras also use these units, but – internally – these correspond to the familiar “gain” in the astronomical CCD detectors. Typically ISO 400 corresponds to a few e-/ADU, while ISO 100 corresponds to 10 – 20 e-/ADU. The exact values can be determined utilizing the discrete nature of the electronic signal, as described below.

The electronic gain of a camera can be determined by taking pairs of images at different exposure lengths of a uniformly illuminated surface source, say a white wall. Pairs of images are required to subtract the bias pattern which exists in all images. The first image taken should result in a fully saturated frame, and subsequent exposures should half the exposure length until a completely dark image is obtained. Several final images with the lens cap on are taken to obtain the bias frame. To calculate the electronic gain for both camera sensitivity settings, a series of pictures were taken for both ISO 100 and 400 settings. Figures 5.3 illustrate the setup for the electronic gain tests. For completeness a itemized list of the complete test setup is described below:

Electronic Gain Test Setup:

1) Aim camera at close range at a uniformly illuminated white screen
2) Place camera in manual mode. This will ensure that halving exposure lengths will uniformly reduce image intensity. If camera is set on an automatic setting it will adjust the aperture setting to capture an optimal image.
3) Set the camera f/ratio to be between 5.6 and 8. Find an exposure length to acquire an image that is just fully saturated for each ISO level tested. This exposure length was determined to be 1/10 seconds for ISO 100 and 1/40 seconds for ISO 400.
4) Ensure camera is focused at infinity (wall is out of focus).
5) Take two identical images in rapid succession starting with exposures lengths specified in step 4.
6) Double shutter speed and take another pair of exposures. Continue taking pairs of images, doubling shutter speeds, until images are dark.
7) Take six bias exposures of 1/100s exposure length with camera lens cap on and uniform light source and room lights off.
8) Perform steps 1) to 7) for ISO settings of 100 and 400.

a)

b)

Figure 5.3: Electronic gain test setup. a) The Canon camera, light source and white screen; b) Camera with view finder blocked.

5.3. Data Reductions

For the Canon camera, every image was taken in a RAW format and subsequently converted into a FITS format using an image processing software, IRIS. This step was not needed for the Electrim camera saving images in FITS. Once in a FITS format, all data reductions were also conducted using the IRIS software.

5.3.1. Electronic Gain

a) Extract all images to Colour Filter Array (CFA) format. This produces a black and white image which shows the signal received by each of the pixels.
b) Convert all CFA images to RGB format, then separate the image into the three colour planes. Only the red plane will be used for all subsequent data reduction.
c) Create a master bias frame for each ISO setting by adding all N bias frames and dividing result by N.
d) Subtract master bias frame from each image of white screen (science frame)
e) Compute the median signal intensity (in ADU) from a central pixel crop from each resulting science frame.
f) Subtract each pair of identical images (same exposure length and ISO) from each other. The resulting image will contain only the readout noise.
g) Calculate the standard deviation from a central pixel crop of the resulting image. Square the standard deviation to obtain variance, and divide by 2 to get the variance for 1 frame.
h) Plot variance vs. signal intensity.
i) The inverse of the slope of the resulting linear relationship between variance and mean signal intensity is the electronic gain of the camera. Units of electronic gain are e-/ADU.
j) Repeat steps a) to h) for each ISO setting.

5.3.2 Readout Noise

Calculating the readout noise only requires the use of the bias frames taken during the test described in section 5.2.1: Dark frame and Bias frame, as well as the electronic gain, as calculated in section 5.3.1. The procedure for calculating the readout noise is described below. Note that since the bias frames are only black and white in nature, conversion from RAW to CFA was required, unlike the previous section where a subsequent conversion to RGB was required..

a) Average all five bias frames taken for each ISO setting at each temperature step to obtain a master bias frame. This averaging will improve the signal to noise ratio, thus determining the bias pattern with a higher precision.
b) Subtract one bias frame from the average bias frame. The resulting image will only contain the readout noise.
c) Compute the standard deviation in ADU from a central crop of pixels from the image.
d) Multiply the electronic gain calculated in the previous section by the standard deviation to obtain the readout noise in electrons.

5.3.3 Dark Current Signal and its Noise

At this point it is useful to restate our main assumption: The dark signal may not be representative for more complex cameras and may be removed in real time by their software. Its direct measurement may give values artificially low. For that reason we carefully determine the total noise and then the dark current noise as an indirect measure of the dark current signal.

Calculating the dark current requires the use of the dark frames (exposure lengths greater than 1/4000 seconds) taken during the test described in previous sections. The procedure for calculating the readout noise is described below.

1) Decode all RAW dark frames into CFA
2) Subtract the master bias from of relevant temperature from each dark frame
3) Subtract one dark frame from another. The resulting image contains only dark noise and readout noise.
4) To isolate the amount of dark noise, use the formula:

$$DarkNoise = \sqrt{(TotalNoise)^2 - (ReadoutNoise)^2}$$

5) Divide the dark noise by square root of two to get noise in 1 frame. Convert dark noise to electrons by using the electronic gain determined for each ISO.
6) Square the noise value and divide by duration of dark exposure to obtain the dark current signal in units electrons per second per pixel (e-/s/pixel).

5.4 Results of measurements

5.4.1 Electronic Gain

The gain as well as the readout noise can be obtained from the linear relationship which relates the variance increase to the signal according to:

$$Variance = (1/ElectronicGain)*(MedianSignalIntensity) + (\mathrm{Re}\,adoutNoise)^2$$

The electronic gain is the inverse of the slope of these relationship. Figure 5.4 shows an actual dependence for the Canon camera. This procedure also is able to give a rough indication of the readout noise at these ISO levels. A more accurate calculation of the readout noise, however, can be obtained by subtracting two bias frames from each other and will thus be discussed in Section 5.2. Table 5.1 contains the electronic gain values as determined by us.

Table 5.1 - Electronic Gain Results

ISO Setting	Electronic Gain (e-/ADU)
Canon ISO100	10.49
Canon ISO400	2.52
Electrim gain#1	125
Electrim gain#4	28

Note that the Electrim camera nominal specifications are: readout 10 e-, dark current 20 e-/s/pix. These were not measurable at the gains available in the provided camera.

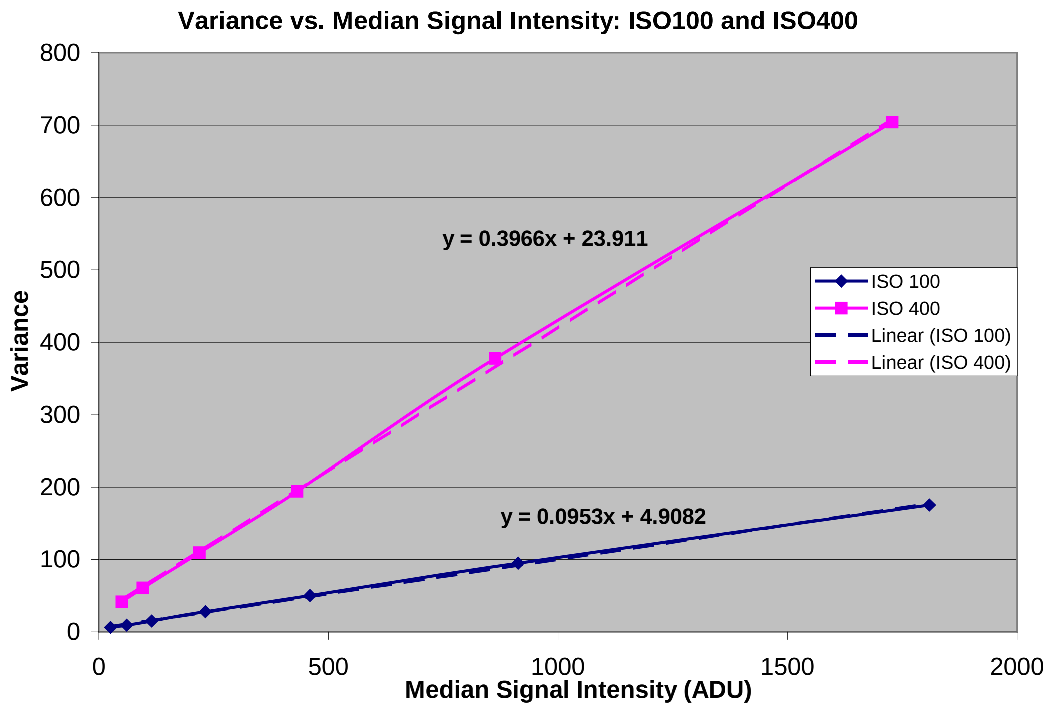

Figure 5.4: The linear dependence of the signal variance on the signal intensity is used to determine the gain as well as an estimate of the readout noise. Results for the Canon camera.

5.4.2 Readout Noise

As described in Section 5.3.2, the readout noise is calculated by multiplying the electronic gain by the standard deviation of a frame which results from the subtraction of a bias frame from the master bias frame. The standard deviation and readout noise results for the six temperature steps between –20°C and 30°C are shown in table 2.0.

Table 5.2: Canon camera. The readout noise at two gain values.

ISO Setting	Temperature (C)	Standard Deviation	Readout Noise (e-)
100	-20	1.6	16.8
	-10	1.6	16.8
	0	1.6	16.8
	10	1.6	16.8
	20	1.7	17.8
	30	1.6	16.8
400	-20	4.1	10.3
	-10	4.1	10.3
	0	4.1	10.3
	10	4.1	10.3
	20	4.1	10.3
	30	4.1	10.3

Terry Lovejoy (2004a,b) reported results for the Canon camera set at ISO 800: Readout Noise Standard Deviation: 7.3 ADU, Electronic Gain: 1.33 e-/ADU and thus Readout Noise = 7.3*1.33 = 9.7e-/ADU. It appears that the readout noise may decrease slightly with higher values of ISO (smaller number of e-/ADU). The decrease is relatively moderate (compare this with 10.3 e- for ISO 400), but this advantage is somewhat illusory as then the noise is oversampled and the dynamic range of the image much reduced. The tendency to set cameras to high “sensitivity” is a common tendency among the amateurs (who are very knowledgeable otherwise). This common trap should be avoided in the design of BRITE.

5.4.3. Dark Noise and Signal

As mentioned before, the dark current signal was evaluated indirectly, through the dark noise, as described in Sec.5.3.3. Thus we found first:

$$DarkNoise = \sqrt{(TotalNoise)^2 - (ReadoutNoise)^2}$$

and then the dark current (rate of the dark signal build-up) from

$$DarkCurrent = DarkNoise^2 / ExpLength$$

The results are shown in the tabular form in Table 5.A.1 and in graphic form in Figures 5.5 and 5.6. The dark signal is barely noticeable for temperatures below 10C, and exposure lengths below 60 seconds. The typical signals are at the level of <1 electron per pixel per second for temperatures approximately 25C.

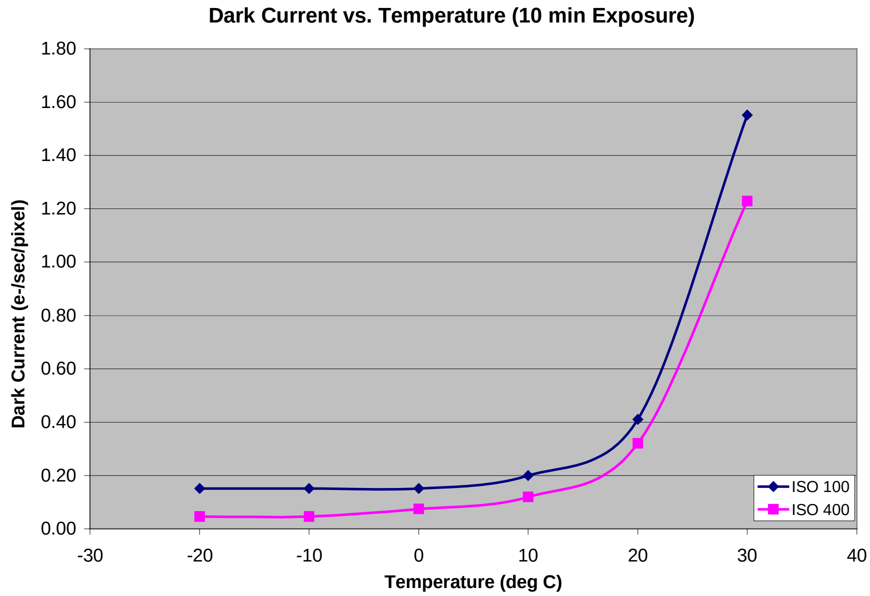

Figure 5.5: The dark current (in electrons per pixel per second) measured from 10 minute exposures.

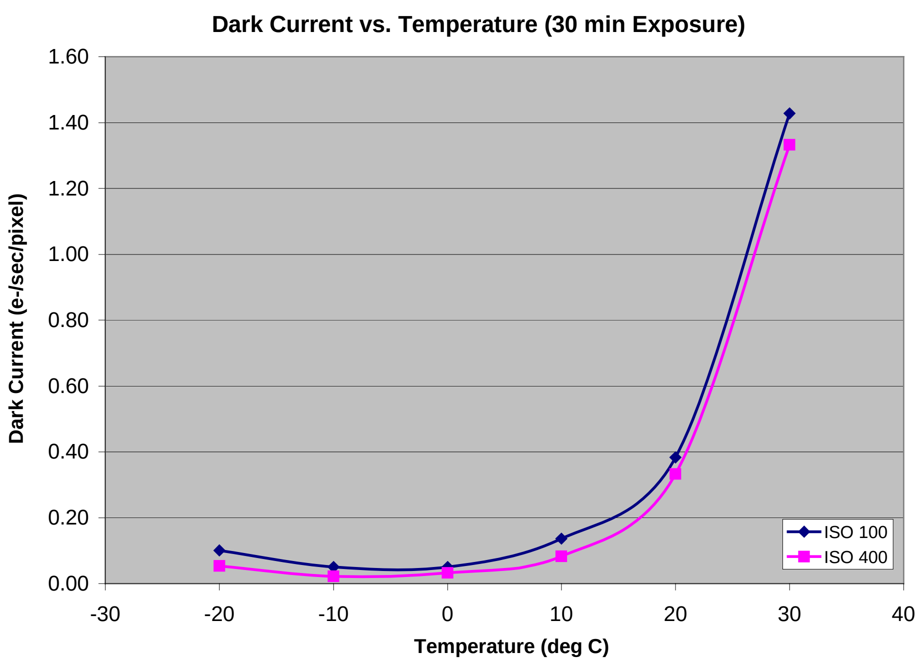

Figure 5.6: The same as in Figure 5.5, but with the dark current measured from 30 minute exposures.

Although the ISO 400 data appear to be slightly better than those for ISO 100, the difference is not significant in that systematic errors in our gain measurements at a level <10% can explain these differences.

Our results agree with those of Lovejoy (2004a,b) who reported a value of 0.9e-/s/pixel of dark current at 27C, for an image duration of 5 minutes at ISO 800. Our estimates are slightly higher (around 1.0 e-/s/pix), but within the margin of errors. Besides, the cameras do not have to be identical.

Appendix 5.A.1: Canon Thermal Tests

Canon camera: Total noise in ADU (ISO 100)

Temp	1800 sec	600 sec	60 sec	10 sec	1 sec
-20 C	2.05	1.84	1.84	-	-
-10 C	1.84	1.84	1.77	-	-
0 C	1.84	1.84	1.77	-	-
+10 C	2.19	1.91	1.91	1.77	1.77
+20 C	2.97	2.19	1.77	1.77	1.77
+30 C	5.09	3.32	1.97	1.84	1.77

Canon camera: Total noise in ADU (ISO 400)

-20 C	5.66	4.60	4.53	-	-
-10 C	4.81	4.60	4.53	-	-
0 C	5.09	4.88	4.60	-	-
+10 C	6.36	5.30	4.60	4.53	4.53
+20 C	10.54	6.86	4.74	4.60	4.60
+30 C	19.86	11.53	-	4.74	4.53

Canon camera: Dark signal noise in ADU (ISO 100)

Temp	1800 sec	600 sec	60 sec	10 sec	1 sec
-20 C	1.28	0.91	0.91	-	-
-10 C	0.91	0.91	0.76	-	-
0 C	0.91	0.91	0.76	-	-
+10 C	1.50	1.04	1.04	0.76	0.76
+20 C	2.50	1.50	0.76	0.76	0.76
+30 C	4.83	2.91	1.15	0.91	0.76

Canon camera: Dark signal noise in ADU (ISO 400)

-20 C	3.90	2.09	1.93	-	-
-10 C	2.52	2.09	1.93	-	-
0 C	3.02	2.65	2.09	-	-
+10 C	4.86	3.36	2.09	1.93	1.93
+20 C	9.71	5.50	2.38	2.09	2.09
+30 C	19.43	10.78	-	2.38	1.93

Canon camera: Dark current signal in e-/sec/pixel (ISO 100)

Temp	1800 sec	600 sec	60 sec	10 sec	1 sec
-20 C	0.10	0.15	1.51	-	-
-10 C	0.05	0.15	1.05	-	-
0 C	0.05	0.15	1.05	-	-
+10 C	0.14	0.20	2.00	(6.30)	(63)
+20 C	0.38	0.41	1.05	(6.30)	(63)
+30 C	1.43	1.55	2.42	(9.08)	(63)

Canon camera: Dark current signal in e-/sec/pixel (ISO 400)

-20 C	0.05	0.05	0.39	-	-
-10 C	0.02	0.05	0.39	-	-
0 C	0.03	0.07	0.46	-	-
+10 C	0.08	0.12	0.46	(2.36)	(24)
+20 C	0.33	0.32	0.60	(2.76)	(28)
+30 C	1.33	1.23	-	(3.59)	(24)

Note: Unreliably determined quantities are in parentheses. For the dark current estimates, the best data are for the longest exposures.

5.5 Conclusions

The thermal tests of the Canon camera show that manufacturers of this CMOS detector very successfully solved the problem of the readout noise (10 el/readout), but particularly of the low thermal emission. Even at room temperature, the dark current is at a level of no more than 1 el/sec/pixel. This performance has been observed in thermoelectrically cooled CCD detectors, but never at room temperatures. Thus this important issue appears to be solved, at least for some chip architectures. The Electrim CMOS detector has a larger dark current, but we could not characterize it because of the inadequate software provided with the camera; the factory specifications are: readout noise of 10 el; dark current 20 el/sec/pixel.

Improvement in quality of CMOS detectors in recent months has been stunning. Not only have they grown in size from the 1K-pixel per side to exceed even 3K×4K pixels, but their noise characteristics have also improved; a year ago the readout noise of 100 el and the dark current of 1000 el/sec/pixel were considered as reasonable baseline figures for the BRITE preliminary design. The performance of the latest CMOS detectors far exceeds the initial requirements.

6. PRELIMINARY OPTICAL DESIGN FOR BRITE

6.1. Stock Objective Lenses

In keeping with the low cost nature of nano-satellites, it would be desirable to use off-the-shelf components whenever possible. However, consumer optics, even lenses for high-end consumer cameras, typically exhibit significant asymmetrical aberrations and are subject to compromises that make them ill suited to precision photometry. These lenses also suffer from a great deal of vignetting, or light fall-off at the edge of the field of view that can amount to a 50% signal loss or more. Truncating the diameters of the lens elements in order to save costs typically causes vignetting, but optical designers consider vignetting to be a degree of freedom, clipping light rays to reduce aberrations. The CMOS detector with its limited quantum efficiency (compared to CCDs) makes any vignetting very undesirable. A stock lens for BRITE would likely have to be disassembled and the lens elements remounted in a cell suited to the vacuum of space. Since the threaded retaining rings are typically bonded in place, there is a high probability the lens elements will be damaged in handling. Also, the lens prescription will be proprietary to the manufacturer and unavailable to aid the design of a new cell. The reverse engineering required to rebuild the lens may exceed the cost of a custom lens.

6.2. BRITE Concept Study Lens Design Overview

The BRITE concept study objective resembles the basic Double-Gauss design form where three or more lenses are placed on either side of a central aperture stop (Figure 6.1). In the BRITE objective the last element in the lens group’s primary function is to force the principal rays of the converging light cones to be normal to the focal plane (i.e. *telecentric*). This is accomplished by giving this element more positive refractive power than usual, thus increasingly altering the direction of the principal rays towards the edge of the field of view. While the overall focusing power of the last element is automatically adjusted to constrain the principal rays to be normal to the focal plane, it’s overall shape is varied (i.e. the relative strength of the two surfaces) can be changed during optimization to aid in manipulating the overall image quality.

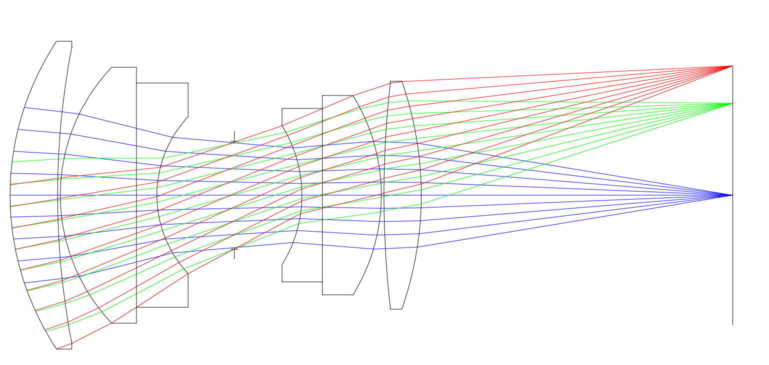

Figure 6.1. Basic Double-Gauss Lens Form

The assumed spectral bandpass was limited to roughly the V-band, 475 nm – 625 nm, however given the desire for large images, the complete spectral range of the detector could possibly be accommodated even with a fast f/2 lens increasing the limiting magnitude. To achieve this performance glass selection was not constrained during optimization, the result is extensive use of high index, conventional substrates. The weight of the lens, 225g, is a direct result of the use of high heavy index substrates. It may be possible to reduce the mass by steering the optimization away from the heavier substrates.

The initial design effort used all radiation hardened substrates and the same Double-Gauss configuration. After some discussion with the BRITE team, it was concluded that the radiation environment (on a sub-Van Allen belt orbit) would not be high enough to justify the cost, and limitations on performance imposed the exclusive use of radiation hardened substrates. The design specifications and performance graphics for this effort is also included at the end of this report.

For this concept study the lens was set at 70mm focal length (scale: 23" per 8 micron pixel) and the overall length of the objective, from the first surface to the focal plane was constrained to be 100mm or less. Optical systems tend to not like being constrained in length; consequently the entire 100mm length budget was used up during optimization.

Tolerance requirements were not investigated during this concept study, however no significant problems are anticipated. Much can be gleaned about the sensitivity of an element to misalignment by observing the path of light rays as they propagate through the system. The only lens element of concern is the last one, which bends the principal rays to be normal to the focal plane. But given the large desired image blur, small displacements of the lens should not have a significant impact on the science observations.

Based on previous communications, the spots sizes for this objective are probably still too small for good sampling, but making them larger and round for all the wavelengths equally will require a significant amount of detail work that will only be meaningful if other issues are addressed that where not touched upon in this concept study. Primary considerations are ghost images, placement of the V-band filter (if used), the objective’s mass and length budget will all have to be factored in to what will likely be the final design. Trade offs can be expected between the desire for a larger aperture, wider field of view and more uniform image blurs. As one gets more “aggressive” with the light, i.e. bigger fields, higher order aberrations take hold off axis to make the spots non-uniform, often quite ugly. Consequently the full, circular field of view was set to only 24 degrees, but the speed was increased to f/2 to increase the signal.

Increasing the image spread for better sampling will decrease the limiting magnitude, but will improve the image sampling and thus precision of photometric measurements. It was suggested early on during team discussion to use, or induce, wandering of the star image on the detector to average out pixel variations in sensitivity. At that time it was unclear how much aberration would be induced by constraining the principal rays to be normal to the focal plane. The concern was that most of the image blur budget would be used up in the lens; it would appear that this is not the case. If further image blurring is anticipated due to possible nanosatellite pointing instability, a case could be made for the lens to form tighter images to increase the expected limiting magnitude.

The design presented here is based on a the aperture of diameter of 35 mm. This is more than assumed in the design of BRITE where an aperture of 25 mm is considered adequate to reach the scientific goals. The design can be easily scaled down to 25mm, however, a larger opening will permit reaching fainter magnitudes and will improve the signal-to-noise ratio for the bright stars, so it would be definitely advantageous. The design is entirely free of vignetting, insures similar angle of incidence of light over the whole area of the detector and attempts to produce similar, if relatively large, images.

6.3. BRITE Concept Study Lens Design Details – Conventional Substrates

Fl	70 mm
Aperture	35mm
Speed	f/2
Bandpass	V-Band (roughly - 475 nm to 625 nm)
Overall length	100 mm (constrained value)
Field of view	24 degrees
Rim ray – half angle	27 degrees (as defined by the f/#)
Image circle	29 mm
Distortion	0.9% (star centroid is 0.13 mm closer to the center of the field than ideal)
Vignetting	0%
Mass	225g (lens components only)

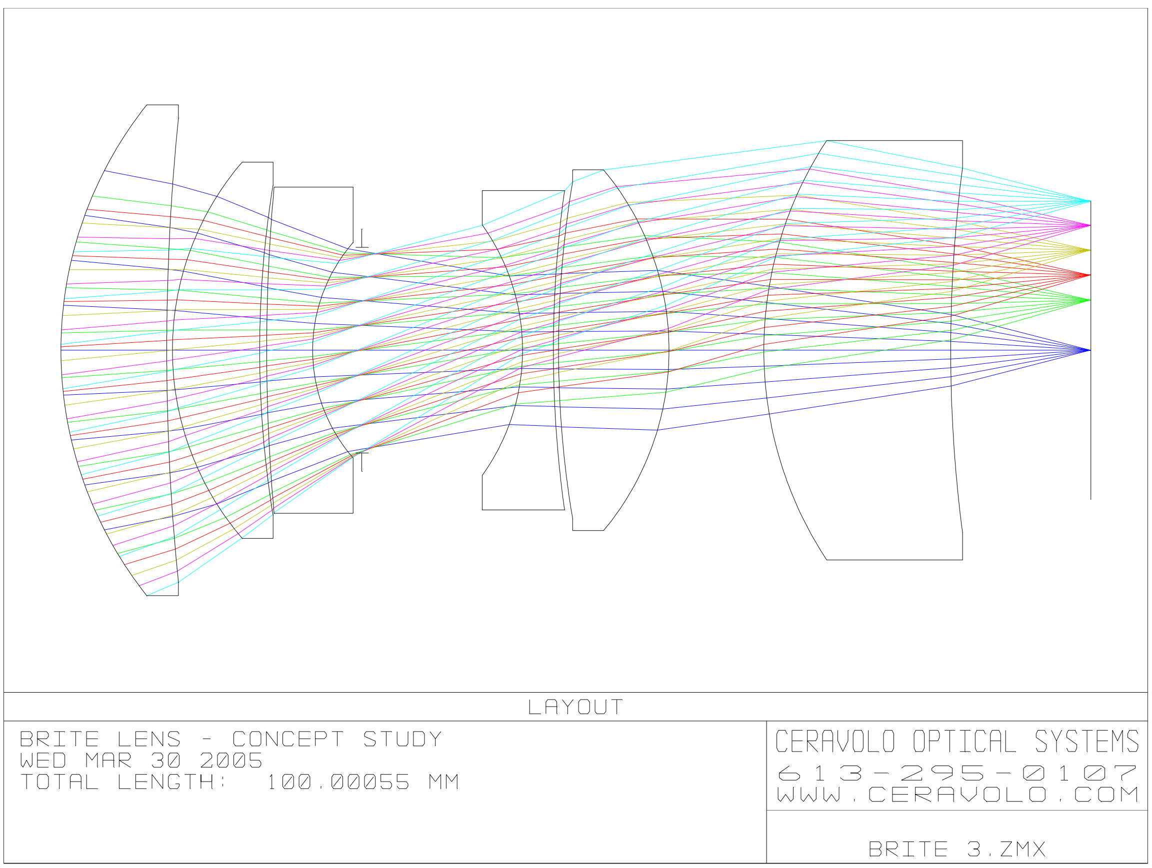

Figure 6.2. The basic preliminary design of the lens telescope for BRITE.

SURFACE DATA SUMMARY:

Surf	Type	Radius	Thickness	Glass	Diameter	Conic
OBJ	STANDARD	Infinity	Infinity		0	0
1	STANDARD	38.4355	10.27344	LAKN7	47.7969	0
2	STANDARD	226.3637	0.5497772		45.2162	0
3	STANDARD	28.18051	8.47262	LAK21	36.65431	0
4	STANDARD	100.2458	0.6828719		32.14466	0
5	STANDARD	175.3725	4.464158	F2	31.78705	0
6	STANDARD	15.99142	4.76744		21	0
STO	STANDARD	Infinity	15.60693		20.03183	0
8	STANDARD	-20.95766	2.99974	F5	24.38839	0
9	STANDARD	112.2007	0.4995537		31.10034	0
10	STANDARD	99.1141	10.72358	N-LAK7	32.82305	0
11	STANDARD	-27.46944	9.210198		35.13235	0
12	STANDARD	37.24893	18.14234	N-LAK33A	40.85682	0
13	STANDARD	137.9547	13.60791		35.47062	0
IMA	STANDARD	Infinity			29.08388	0

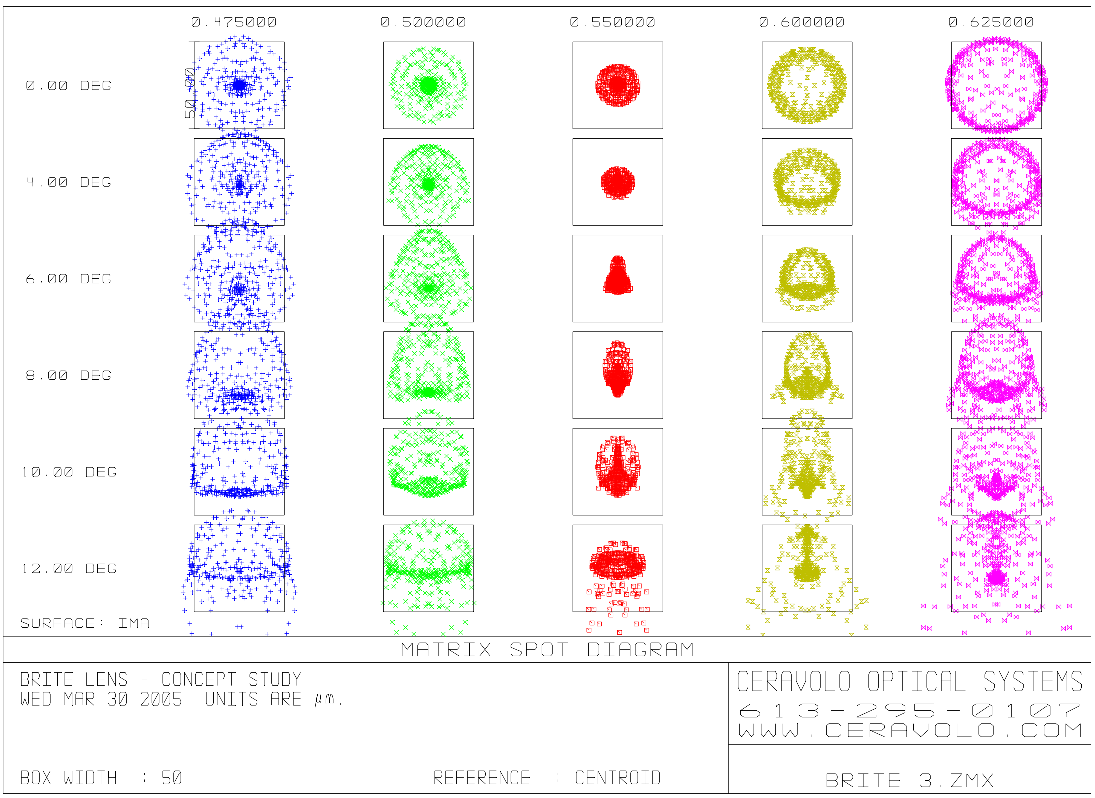

Figure 6.3. The spot diagrams for the design presented above. The squares are 50x50 microns in size. The 5 wavelength regions are given as columns in this picture (475, 500, 550, 600, 625 nm).

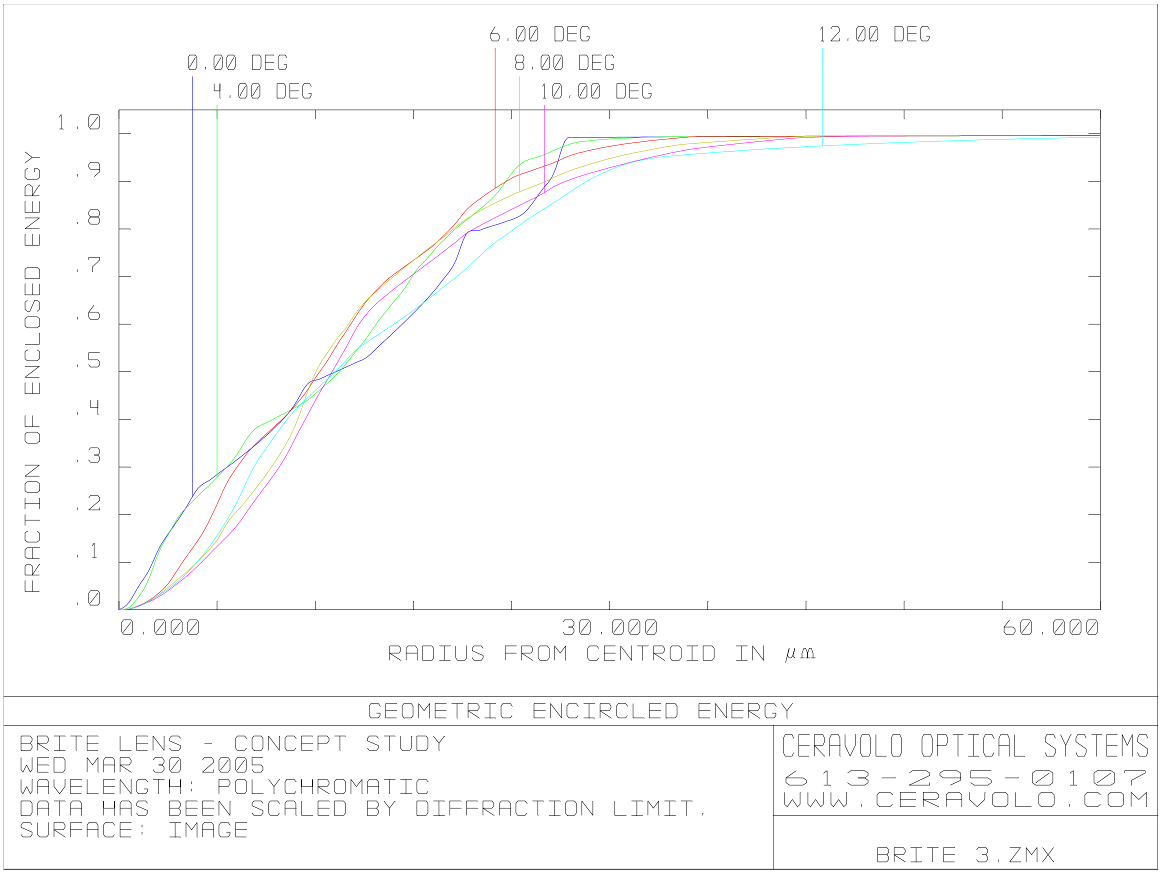

Figure 6.4. The energy concentration diagrams for the design presented above, for 6 radial distances from the optical axis: 0, 4, 6, 8, 10 and 12 degrees.

6.4. BRITE Concept Study Lens Design Details - Radiation Hardened Substrates

Fl	70 mm
Aperture	35mm
Speed	f/2
Bandpass	V-Band (roughly - 475 nm to 625 nm)
Overall length	100 mm (constrained value)
Field of view	24 degrees
Rim ray – half angle	27 degrees (as defined by the f/#)
Image circle	29 mm
Distortion	1.4 %
Vignetting	0%
Mass	115g (lens components only)

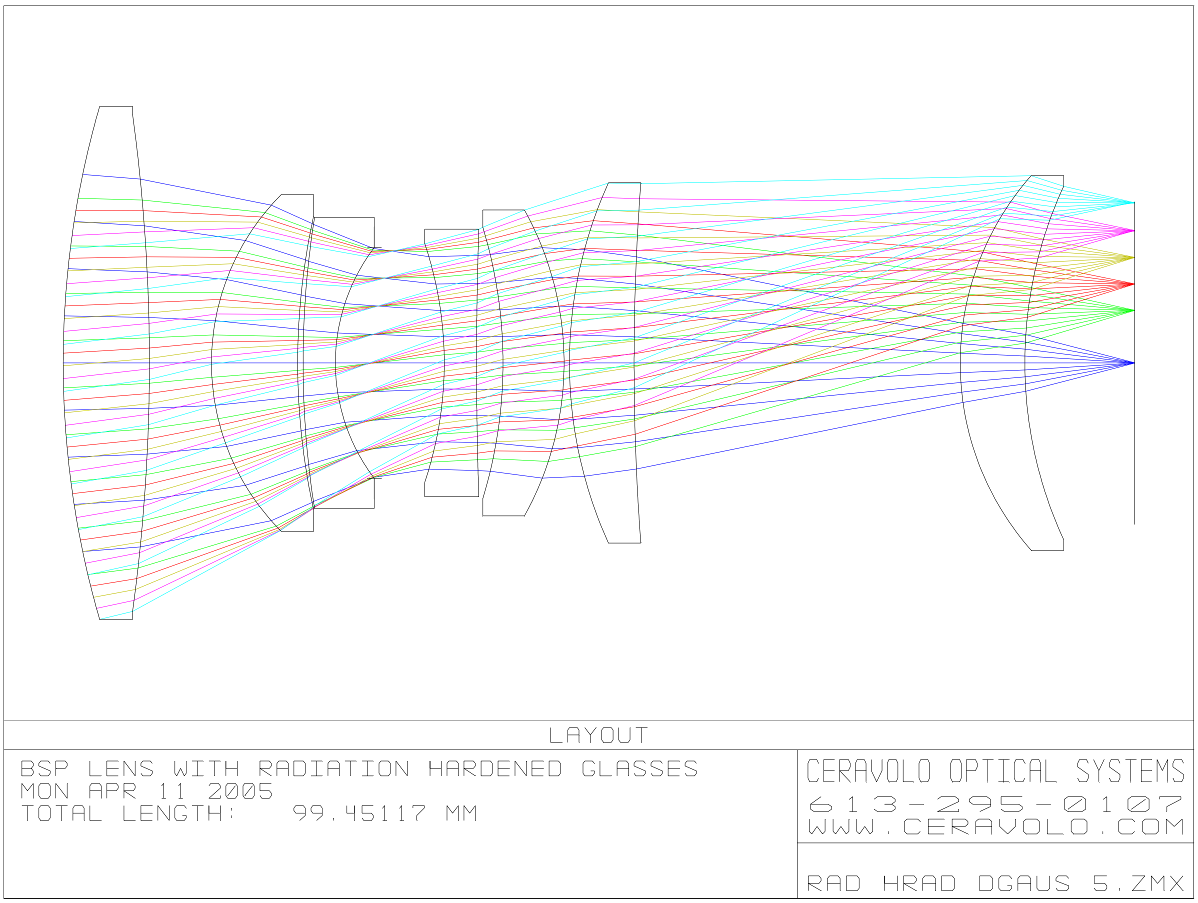

Figure 6.5. The preliminary design of the lens telescope for BRITE utilizing radiation hardened glasses.

SURFACE DATA SUMMARY:

Surf	Type	Radius	Thickness	Glass	Diameter	Conic
OBJ	STANDARD	Infinity	Infinity		0	0
1	STANDARD	85.51222	8	F2G12	47.6144	0
2	STANDARD	-171.2381	5.767383		46.13557	0
3	STANDARD	22.10779	8	LAK9G15	31.26362	0
4	STANDARD	63.54292	0.4997956		27.21355	0
5	STANDARD	86.58783	3	SF6G05	27.03173	0
6	STANDARD	17.70513	3.603824		21.41281	0
STO	STANDARD	Infinity	6.499122		21.41286	0
8	STANDARD	-34.76104	2.999997	F2G12	22.16023	0
9	STANDARD	368.8309	2.452489		24.83009	0
10	STANDARD	-43.2805	5.670332	SF8G07	25.1908	0
11	STANDARD	-29.25765	0.5000024		28.39622	0
12	STANDARD	40.42251	6	LAK9G15	33.45071	0
13	STANDARD	223.4819	30.27439		33.3371	0
14	STANDARD	26.24894	6	LAK9G15	34.80249	0
15	STANDARD	39.1861	10.18383		32.84274	0
IMA	STANDARD	Infinity			29.92298	0

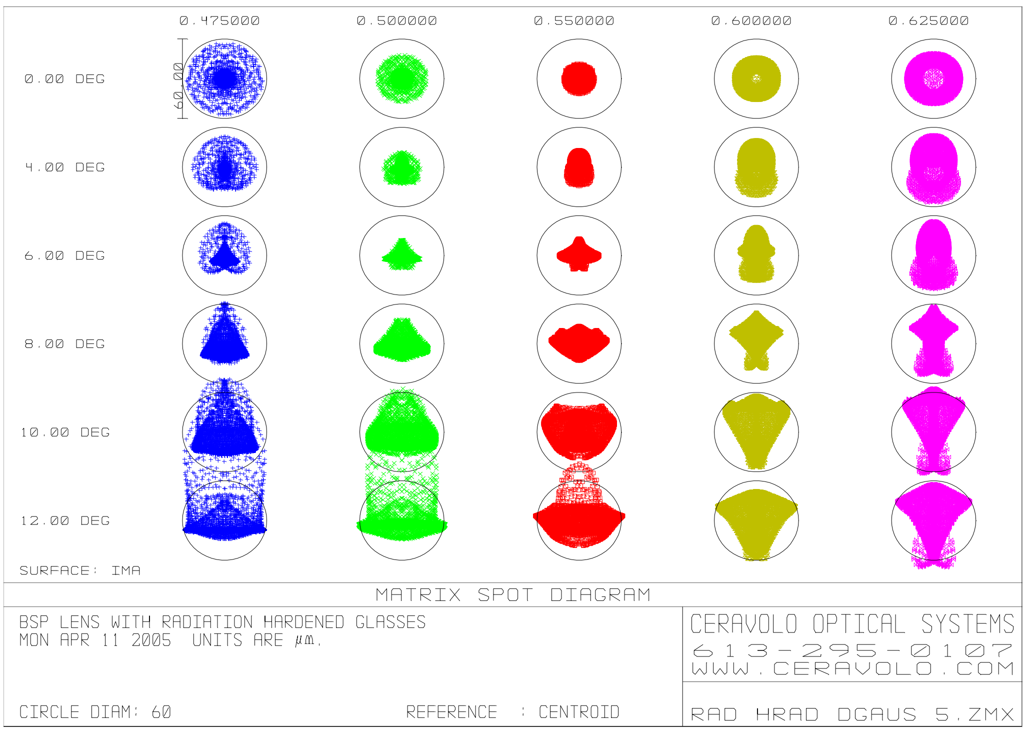

Figure 6.6. The spot diagrams for the design presented above. The squares are 50x50 microns in size. The 5 wavelength regions are given as columns in this picture (475, 500, 550, 600, 625 nm).

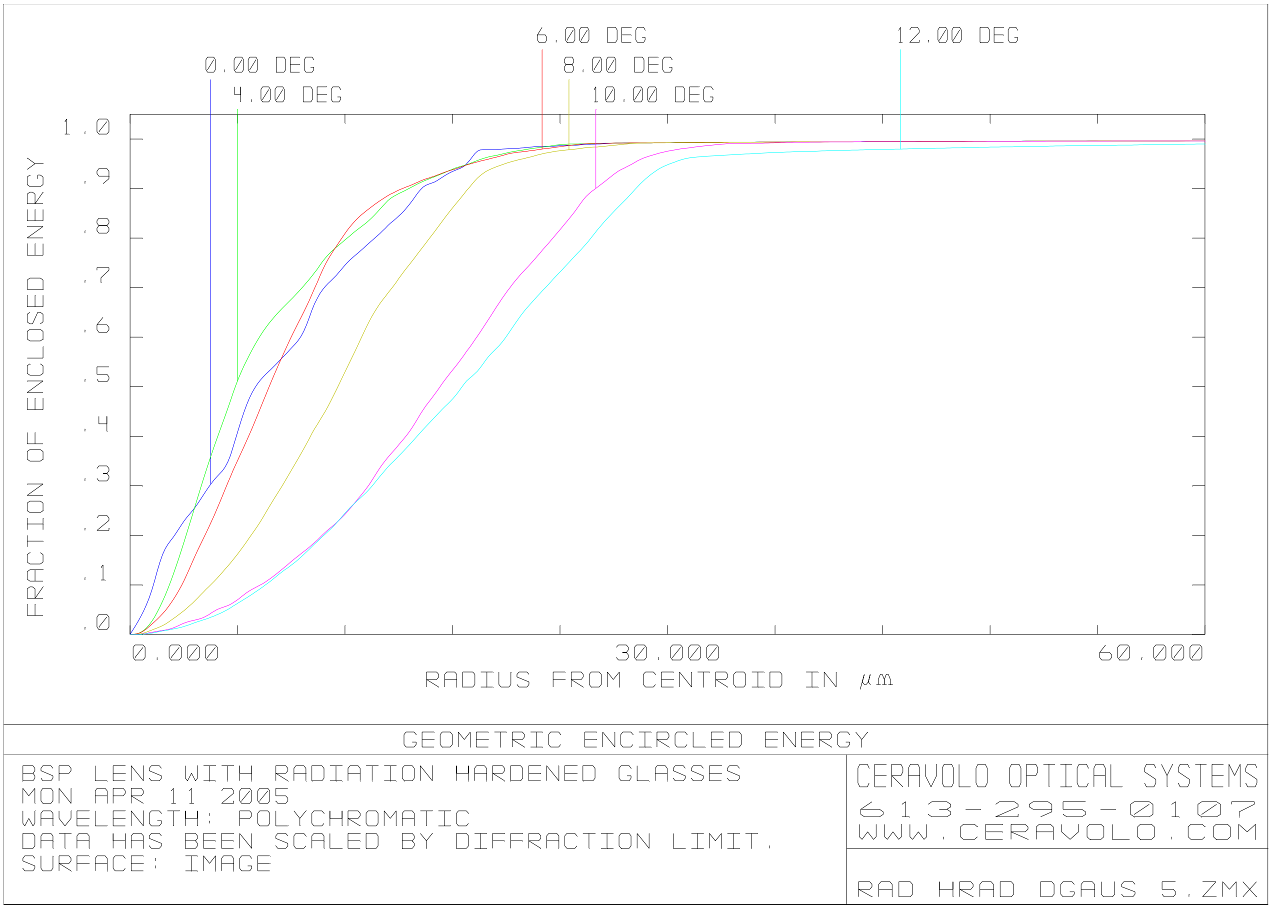

Figure 6.7. The energy concentration diagrams for the design presented above, for 6 radial distances from the optical axis: 0, 4, 6, 8, 10 and 12 degrees.

6.5. BK7 glass and its radioactivity

It has been known for some time that BK7 optical glass, a staple in the optics industry for lens substrates, is mildly radioactive. Many optical systems use BK7 windows or field lenses relatively close to the focal plane. Long integrations with these systems exhibit a higher level of charged particle hits than similar integrations with fused silica elements.

The MOST instrument uses a BK7 field lens approximately 10 mm from the focal plane, and a BK7 Fabry lenslet array immediately above the CCD. Any crown type substrate could have been used for these elements, including fused silica, but BK7 was chosen to filter out the deep UV light. The realized charged particle hit count has not proved to be an issue in the MOST, time resolved, observations. Given the similar observing regimes for BRITE, BK7 glass should not pose a problem if it is incorporated in the lens design. However, excluding BK7 substrate is not expected to pose a serious design constraint.

6.6. Conclusions from the preliminary optical design

CMOS detectors are ideal for the BRITE nano-satellite imaging system because of their low power requirements. The purpose of this part of the study was to investigate the viability of designing an imaging lens ideally suited to CMOS detectors, which lose sensitivity when light strike them at large angles of incidence. The ideal lens' principal rays would be constrained to be normal to the detector across the entire field of view while at the same time exhibiting no vignetting. In this case the imaging rays angle of incidence would be solely defined by the lens focal ratio.

The BRITE lens, limited to the V-band, does not need good image quality; in fact for good photometry the images need to be relatively large (or "apodized", i.e. free from high spatial frequencies) so as to average out the CMOS's pixel-to-pixel variation of sensitivity, mitigate their limited dynamic range and minimize effects of possibly large inter-pixel spacing due to front electrodes. This requirement for relatively large images is advantageous since constraining the principal rays to be normal to the detector, and the desirability of a fast lens invariably introduce image blurring aberrations. The preliminary design presented here gives similar, relatively large images (total energy confined within a 30 micron radius circle) over the whole field of view of 24 degree diameter. With the currently envisaged 8 micron pixels and thus the scale of 23"/pixel for f=70 mm, the image will spread within 7.5 pixel diameter (the100%-energy confinement radius of 3.75 pixels). This results in the Point Spread Function (PSF) sampled by about 45 pixels in two dimensions. It is likely that satellite stabilisation motions with typical *rms* error of about 1 arcmin (corresponding to 2 – 3 additional pixels in the image smear) will result in even larger images. This should insure adequate sampling of the PSF in all points of the field. Commercial lenses with rapidly changing PSF across the field of view and thus uneven image sampling and with strong vignetting cannot be used in BRITE. For the same f/2 lens speed, it would be advantageous to have a system with f = 70mm (as in the presented design) rather than the popular f = 50mm because this leads to a better matching of the image linear and angular scales. If a detector with smaller pixels (say 6 micron) is selected, the whole design may be re-scaled to f=50mm; however, small pixels are not advantageous as they have a smaller charge capacity.

7. SKY OBSERVATIONS USING THE CANON CAMERA

7.1. Observational setup

The Canon camera was used for simple sky imaging tests, to show directly that a lens/CMOS based imaging system is a viable solution of large-angle sky imaging. We used the same DSLR Canon EOS 300D (Digital Rebel) camera as described in the previous sections of this study. The camera is normally sold with a zoom objective (EF-S18-55mm f/3.5-5.6) lens. Instead of this lens, we used a simpler, single-focus Canon lens EF50mm f/1.8 II. This lens, with a focal length of 50 mm and with the opening of slightly over 25 mm diameter was considered as a reasonable approximation of the BRITE optics. As we see below, the lens turned out much poorer than expected.

The Canon camera was mounted on the 1.88m telescope, close to its end and thus close to the dome shutters giving a very large opening angle for imaging. Several images were taken with exposure times of 3, 10 and 30 seconds at the ambient temperature of about 12C, which – possibly – would not be far from the expected working temperature of the BRITE detector. The gain setting was ASA 400 which corresponds to e-/ADU = 2.5.

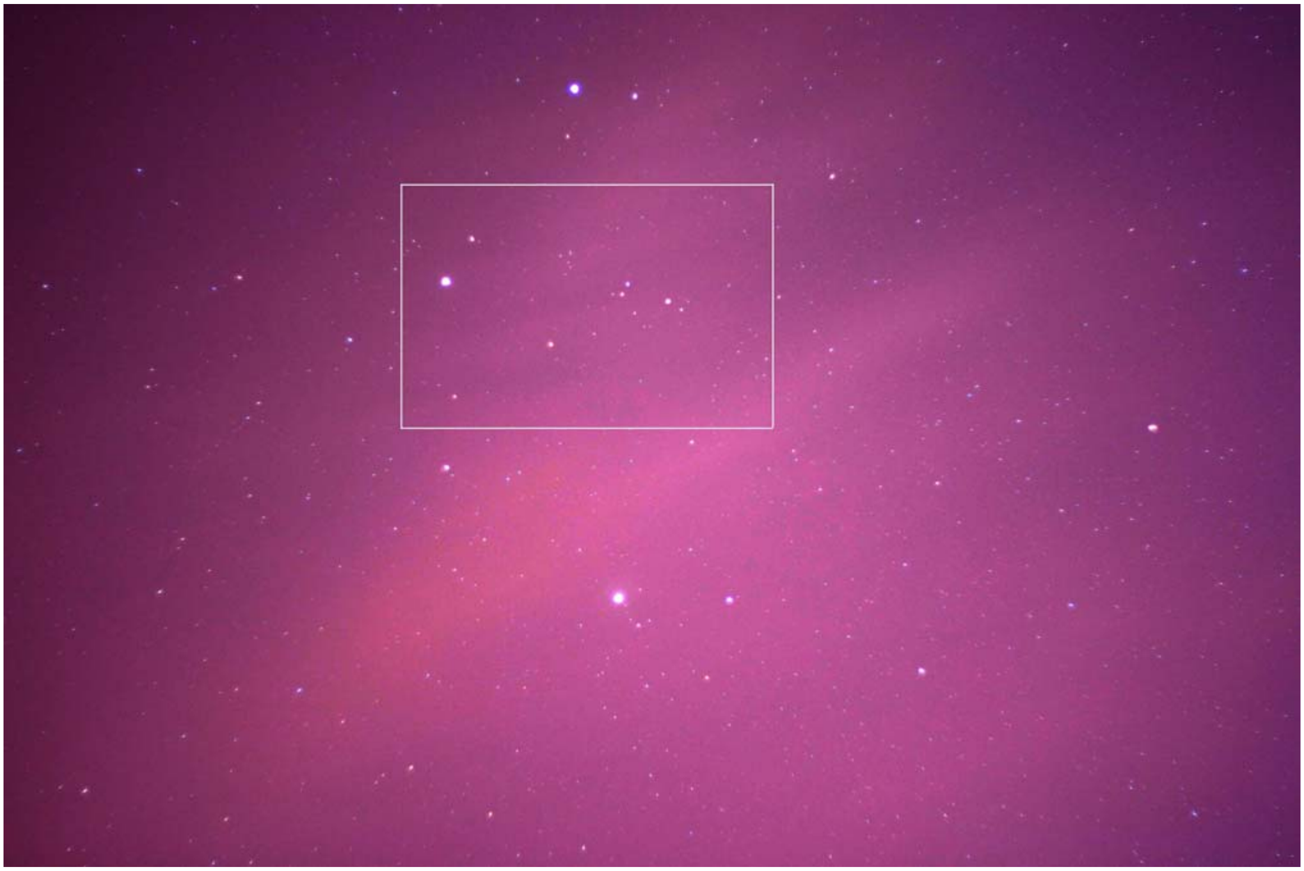

Figure 7.1: A typical whole field accessible to the Canon camera in a 30 second exposure. The images shows a 24 × 16 degree field of Gemini with Saturn below the centre of the image. Castor is in the upper part of the image, while Pollux is in the box marking a magnified field shown in Figure 7.3. Very faint cirrus clouds were present, but most of the brightness variation is due to the Toronto sky projected through the system showing angular sensitivity variations of the CMOS chip (as studied in Section 4), possibly modified by vignetting effects of the 50 mm lens.

The field imaged was that of the Gemini bright stars with Saturn visiting this part of the sky. Figure 7.1. shows the whole field observed. A cut through the field is shown in Figure 7.2 while a sub-field, marked by a box in Fig.7.1. is shown in the Figure 7.3. Pollux is the bright star in the left side of the box.

7.2. Image analysis

The images were taken as normally with a colour camera, but they were converted to B/W fits format in the processing stage. This way, the added counts could better mimic the total output of an un-filtered detector.

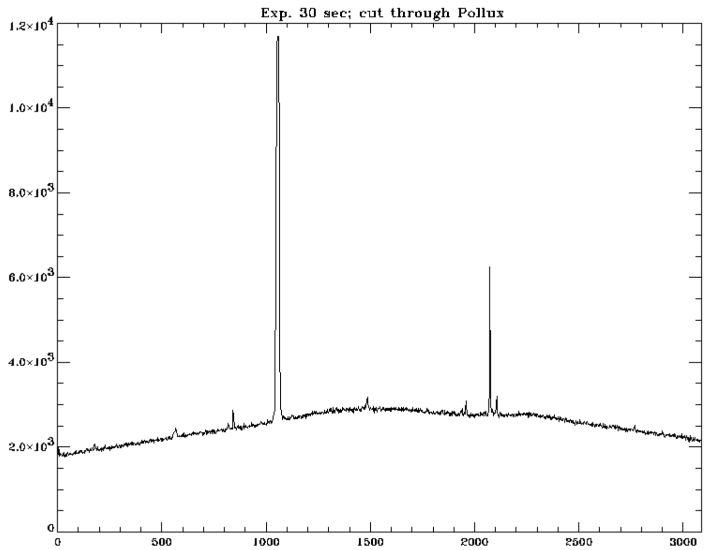

Figure 7.2. A horizontal cross-section passing through a saturated image of Pollux. Note the strong variation of the sky background mostly due to the CMOS angular sensitivity variation, but probably combined with vignetting of the lens.

The camera limitations are very clearly shown in Figure 7.2: (1) The 12-bit (i.e. 4096 level) digitisation of the signal has resulted, after the 3-colour to B/W conversion in a maximum capacity in each channel of slightly over 12,000 level saturation for the image of Pollux; (2) The background shows a rather obvious surface brightness variation across the field, as a function of the distance from the optical axis, with an amplitude of about 35% over the whole ±12 degree range. As was discussed in Section 4, the CMOS detector appears to produce a 15% to 20% variation, so the rest must be due to vignetting in the lens, perhaps coupled with the non-perpendicular incidence of the light on the detector. We note that the images of stars are very poor far from the optical axis so a lens such as the one used would not be acceptable for BRITE.

We took separate dark signal images of the same duration before and after the sky images, but the raw –format images showed only a constant pedestal signal most likely corresponding to the pre-set bias. Thus, it appears that the camera indeed shows an exceptionally low thermal signal, in full agreement with the results presented in Section 5. The main limitation in terms of the background brightness was the bright Toronto sky (currently estimated at 16.5 to 17 mag/arcsec^2; for more information, see http://www.astro.utoronto.ca/DDO/prospective/torontosky.html), possibly combined with a very thin cirrus on this particular night.

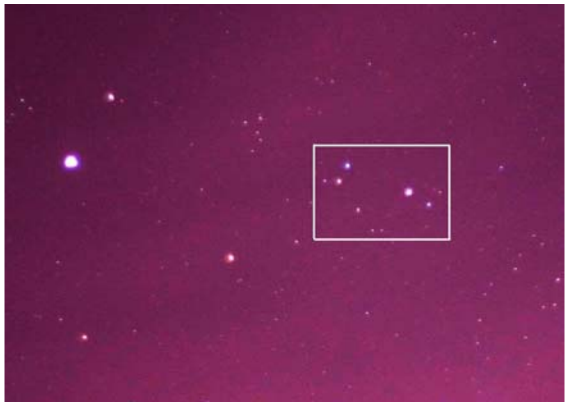

Figure 7.3. The central parts of the image as in Figure 7.4. Note that the faintest object visible in this image (a very small Cassiopeia-like configuration slightly above and left of the centre) are 8 magnitude stars. The bright stars in the box are 4 – 5 magnitude stars; a 2-D representation of this part of the image s shown below.

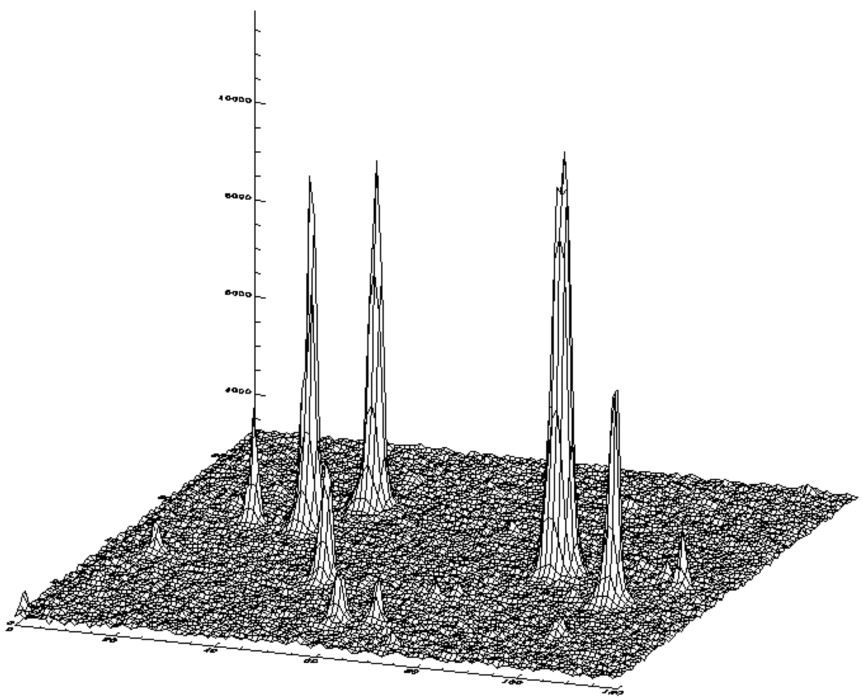

Figure 7.4. A two-dimensional representation of the small centre/right part of Figure 7.3 with stars ranging in brightness from 4 magnitude to the barely detectable 9 magnitude stars. Although the Canon camera was not optimized for precise photometry, it still has a capability of providing relative magnitudes of the three brightest stars with errors smaller than 1%.

7.3. Conclusions

The sky imaging experiments clearly show that a hand-held lens camera, based on an optical/CMOS configuration similar to that envisaged for BRITE, can easily perform precise photometry of stars brighter than 5^{th} magnitude at the error level of about 1%, which is good, but not adequate for BRITE which is planned to provide precision better than 0.1%. To achieve that, the CMOS angular sensitivity variations (discussed in Section 4) must be carefully addressed and the optical system must be well designed to be free of vignetting and with perpendicular illumination of the detector over the whole field, the way as discussed in the description of the preliminary optical design in Section 6. In the design of BRITE, the camera should be very well calibrated for sensitivity variations before the launch, but it a provision must be made for taking flat field images in-orbit to correct for possible sensitivity changes over time.

Current CMOS detectors are sensitive enough and have sufficiently low dark signal to serve for the expected range of stellar magnitudes. To utilize this high sensitivity, the current, commonly encountered limitation of 12-bit converters will require a very careful attention by provision of a sufficiently wide dynamic range of exposure times, typically in the range of 0.1 sec to 100 sec. The 12-bit limitation can possibly be circumvented by external digitization of the output at 14 bits/ADU.

8. CONCLUSIONS OF THE STUDY

We tested two CMOS detector systems, one in a typical hand-held upper-end Canon camera and one in a scientific/industrial camera made by Electrim. We confirmed results of the literature and Internet research presented in Section 2 and added new data on angular sensitivity and thermal noise properties for these cameras (Sections 3, 4 & 5). A preliminary optical design for the BRITE nanosatellite specifically addressing limits on the incidence angle of CMOS detectors in presented in Section 6. Simple sky tests using the Canon camera are described in Section 7.

A CMOS based imaging system for BRITE will have sufficient sensitivity with a large margin. Even without cooling, modern CMOS detectors have dark current so low (as low as 1 electron per second per pixel for temperatures below 20C, though somewhat higher in sensors with different pixel architectures) that this aspect is of little or no concern for the exposures of 10 to 100 seconds in duration which will be used by BRITE. More significant is the dynamic range limitation set by the A/D on-chip converters: the commonly used 10 bits/ADU (1024 levels) conversion is definitely not sufficient; the 12 bits/ADU (4096 levels) in DSLR camera sensors is just marginally adequate, requiring careful adjustment of exposure times. If the overall power budget of the satellite would tolerate that, consideration should be given to a 14-bit external A/D converter.

A rather large difference in angular sensitivity variations has been seen between the Canon and Electrim CMOS detectors. Within the expected angles of incidence of <12 degrees, the former shows a decrease in response by 15 – 20% in the pitch angle and 5% in the yaw angle, whereas the latter shows much smaller effects at <3% level in both rotations. The poor angular performance of the Canon camera is probably due to the presence of the electronic components and micro-lenses in front of the detector, most likely compounded by the Bayer mask & IR filter. These latter filters are absent in the Electrim camera which does have micro-lenses in its Micron-manufactured detector. The IBIS4-14000, sensor which we were unable to test for this study, is expected to have better angular response and larger overall size, without either filters or micro-lenses, but at the expense of higher (though still quite tolerable) dark current.

Sky images taken with a 50mm f/1.8 commercial lens showed that the Canon camera suffers from vignetting-like effects even larger than those expected for the bare detector, at a 20% – 40% level. This is probably due to the presence of the micro-lenses and filters, in combination with the non-perpendicular incidence of the light beam for the standard photographic lens. This is not an insurmountable problem: This study presents a preliminary optical design for BRITE which is free of vignetting and insures perpendicular incidence of light on the detector and adequate sampling of the PSF.

Even if the optical system is designed to be free of vignetting, in-orbit, through-the-lens, flat-fielding procedures should be established in the BRITE design. This will be absolutely necessary to assure a high precision of the BRITE mission as the detector sensitivity may deteriorate over time and may be spatially non-uniform.

An optimum system as envisaged currently for BRITE should have >3000 pixels of 6 – 8 micron per side; this, at the scale of 25″ – 30″/pixel, would give a field of 25 degrees in diameter. Any CMOS detector with the readout noise of <35 el/sec and dark current <100 el/sec/pixel would be sufficient for the purpose. Such detectors are already available commercially. Angular sensitivity variations similar to those reported for the Canon detector would be minimized if the optical system followed the telecentric design principles as described in this Study

It is fortunate that we do not have to select a CMOS detector for BRITE at this stage. The technology is so rapidly evolving that we simply cannot recommend any particular type of the detector. What is obvious, however, is that the detector should be selected to be free of the Bayer colour matrix and any IR-blocking filters (possibly also of micro-lenses). The best solution would be to establish a close collaboration with a CMOS manufacturer. Many detector building companies are currently exploring switching from the CCD to CMOS as the latter offer almost equally excellent sensitivity performance with lower power requirements, low thermal noise and ease of computer interfacing, all this without the charge-transfer penalty. A somewhat unwelcome direction of the CMOS detector evolution is towards very small pixels, below what may be the optimum size for our application of about 6 to 8 microns; this evolution leads to a decrease of the charge well and constraints on the optical design for wide-field applications. It is likely that of the image size of 24 ×36 mm sampled at 6 or 8 microns will become a *de facto* standard of CMOS detectors in the near future. Any detector of such type would serve well for BRITE.

LITERATURE

Buil, C. 2004a, http://astrosurf.com/buil/d70v10d/eval.htm
Buil, C. 2004b, http://astrosurf.com/buil/20d/20dvs10d.htm
Jakl, E. A. 1999, http://home.pacific.net.hk/~kcyeung/ccd-cmos.pdf
Janesick, J.R. 2001, `"Scientific Charge-Coupled Devices", (SPIE:Bellingham, WA), p.622
Janesick, J. and Putnam, G. 2003, Ann. Rev. Nucl. Part. Sci., 53, 263
Lovejoy, T. 2004a, http://members.ozemail.com.au/~lovejoyt/300d.htm
Lovejoy, T. 2004b, http://www.pbase.com/terrylovejoy/canon_1d_mk2}
Manago, N. and Sasaki, M. 2004, http://www.icrr.u-tokyo.ac.jp/~ashra/workshop/040108/viewgraph/GRB-opf.pdf
Meynants, G, Scheffer, D., Dierickx, B., Alaerts, A. 2004, "A 14 MPixel 36 × 24mm^2 Image Sensor", Electronic Imaging, San Jose, 21 Jan 2004 ; SPIE Proceedings Vol. 5301, p.168